

A KINETIC STUDY OF SOME LIGAND SUBSTITUTION REACTIONS

A Thesis

Presented to the

Faculty of the Department of Chemistry

College of Arts and Sciences

University of Houston

In partial fulfillment  
of the requirements for the degree  
Master of Science

by

Chin-tung Lin

June, 1967

400849

A KINETIC STUDY OF SOME LIGAND SUBSTITUTION REACTIONS.

A Thesis

Presented to the

Faculty of the Department of Chemistry

College of Arts and Sciences

University of Houston

In partial fulfillment

of the requirements for the degree

Master of Science

by

Chin-tung Lin

June, 1967

## ACKNOWLEDGEMENTS

I am deeply indebted to my major Professor, Dr. John L. Bear, for his brilliant guidance, enthusiastic assistance and financial support of this work. I also wish to express my sincere thanks to Dr. Anthony J. Graffeo and Dr. Edward Chen for their many invaluable discussions.

A KINETIC STUDY OF SOME LIGAND SUBSTITUTION REACTIONS

An Abstract of

A Thesis

Presented to the

Faculty of the Department of Chemistry

College of Arts and Sciences

University of Houston

In partial fulfillment

of the requirements for the degree

Master of Science

by

Chin-tung Lin

June, 1967

## ABSTRACT

The rate constant for the formation and dissociation of the one-to-one complexes of nickel with malonate and succinate ligands and magnesium with oxalate ligand have been determined by a pressure-jump technique. The rates were determined at different temperatures and the activation parameters calculated. The results indicate that within experimental error there is no change in the activation parameters resulting from a change in properties of the ligand and they are consistent with a model in which the rate-determining step is the elimination of a water molecule from the inner hydration shell of the metal ion.

## TABLE OF CONTENTS

CHAPTER	PAGE
ACKNOWLEDGEMENTS.....	i
ABSTRACT.....	ii
I. INTRODUCTION.....	1
II. THEORY.....	6
A. The Relaxation Time and the Rate Constant.....	6
B. Kinetics of Fast Reactions in Solution.....	13
C. Nature of the Pressure-Jump Method.....	17
III. EXPERIMENTAL.....	21
A. Apparatus.....	21
B. Preparation of the Solutions.....	25
IV. RESULTS AND DISCUSSIONS.....	34
REFERENCES.....	63

## LIST OF TABLES

TABLE	PAGE
I.	Relaxation Times and $f(c)$ for Nickel(II) Malonate at 14.5°C ( $\mu \rightarrow 0$ )..... 36
II.	Relaxation Times and $f(c)$ for Nickel(II) Malonate at 23.5°C ( $\mu \rightarrow 0$ )..... 37
III.	Relaxation Times and $f(c)$ for Nickel(II) Malonate at 32.5°C ( $\mu \rightarrow 0$ )..... 38
IV.	Relaxation Times and $f(c)$ for Nickel(II) Succinate at 12.5°C ( $\mu \rightarrow 0$ )..... 39
V.	Relaxation Times and $f(c)$ for Nickel(II) Succinate ( $\mu \rightarrow 0$ )... 40
VI.	Relaxation Times and $f(c)$ for Magnesium Oxalate at 12.8°C ( $\mu \rightarrow 0$ )..... 41
VII.	Relaxation Times and $f(c)$ for Magnesium Oxalate ( $\mu \rightarrow 0$ )..... 42
VIII.	Rate Constants and $C_0$ for Nickel(II) Malonate..... 47
IX.	Rate Constants and $f(c)$ for Nickel(II) Succinate..... 48
X.	Rate Constants and $f(c)$ for Magnesium Oxalate..... 49
XI.	Rate Constants $k_{34}$ for the Formation of Inner-Sphere Coordination Complexes between Nickel and Various Ligands.. 53
XII.	Kinetic Data for the Nickel(II) Malonate Formation at 23.5°C ( $\mu \rightarrow 0$ )..... 54
XIII.	Kinetic Data for the Nickel(II) Succinate Formation at 21.5°C ( $\mu \rightarrow 0$ )..... 55

LIST OF TABLES CONTINUED

TABLE		PAGE
XIV.	Kinetic Data for the Magnesium Oxalate Formation at 12.8°C ( $\mu \rightarrow 0$ ).....	57
XV.	Substitution of Inner-Sphere Aquo Complexes.....	58
XVI.	Entropies of Activation of the Rate-Limiting Step.....	60

## LIST OF FIGURES

FIGURE		PAGE
1.	The Reciprocal Time Ranges of Relaxation Techniques.....	2
2.	Multiple Step Complex Formation Mechanism.....	4
3.	Relaxation Response Following a Rectangular Step Function.....	8
4.	The Pressure-Jump Apparatus.....	22
5.	The Conductivity Cell.....	23
6.	Pressure-Jump (Without Chemical Relaxation Process).....	26
7.	Experimental Relaxation Curve for Nickel Malonate.....	27
8.	Experimental Relaxation Curve for Nickel Malonate.....	28
9.	Experimental Relaxation Curve for Nickel Succinate.....	29
10.	Experimental Relaxation Curve for Magnesium Oxalate.....	30
11.	Measurement of the Relaxation Time from the Oscillogram Pattern.....	31
12.	Concentration Dependence of the Relaxation Time for Nickel Malonate.....	44
13.	Concentration Dependence of the Relaxation Time for Magnesium Oxalate at 13°C.....	45
14.	The Temperature Dependence of $k_f$ .....	46

CHAPTER I.  
INTRODUCTION

## INTRODUCTION

In recent years new techniques for the investigation of very rapid reactions in solution have become available. As a consequence, a detailed study of the elementary steps involved in a reaction and the combination of these steps in the overall mechanism is now possible. Rate constants can now be determined over the entire time range from slow reactions accessible by conventional techniques to the fastest reactions conceivable from the current theories.

For a long time almost all our knowledge was restricted to two time ranges that are separated by about ten orders of magnitude. One is the range of chemical kinetics, the lower limit of which is about one second, and the other, the range of spectroscopy, the limits of which are  $10^{-10}$  and  $10^{-15}$  second. The gap between these two time ranges has been subjected to study only recently. Some of the new techniques used to study chemical reactions in this region are shown in Figure 1. Several of these are perturbation techniques that are classified as relaxation methods (1) such as the temperature-jump (2), the pressure-jump (3,4), and the semiclassical ultrasonic absorption techniques (5).

In all relaxation methods a chemical equilibrium is perturbed by a rapid change in one of several possible external parameters (electric field intensity, temperature, or pressure). Then there is a finite time lag while the system approaches the new position of equilibrium governed by the new set of external parameters. This time lag is related to the rate constants of the forward and reverse reactions. Changes in the solvent structure caused by a perturbation proceed much

## FIGURE 1

## THE RECIPROCAL TIME RANGES OF RELAXATION TECHNIQUES

C = Classical Range

E = Electric Field

F = Flow

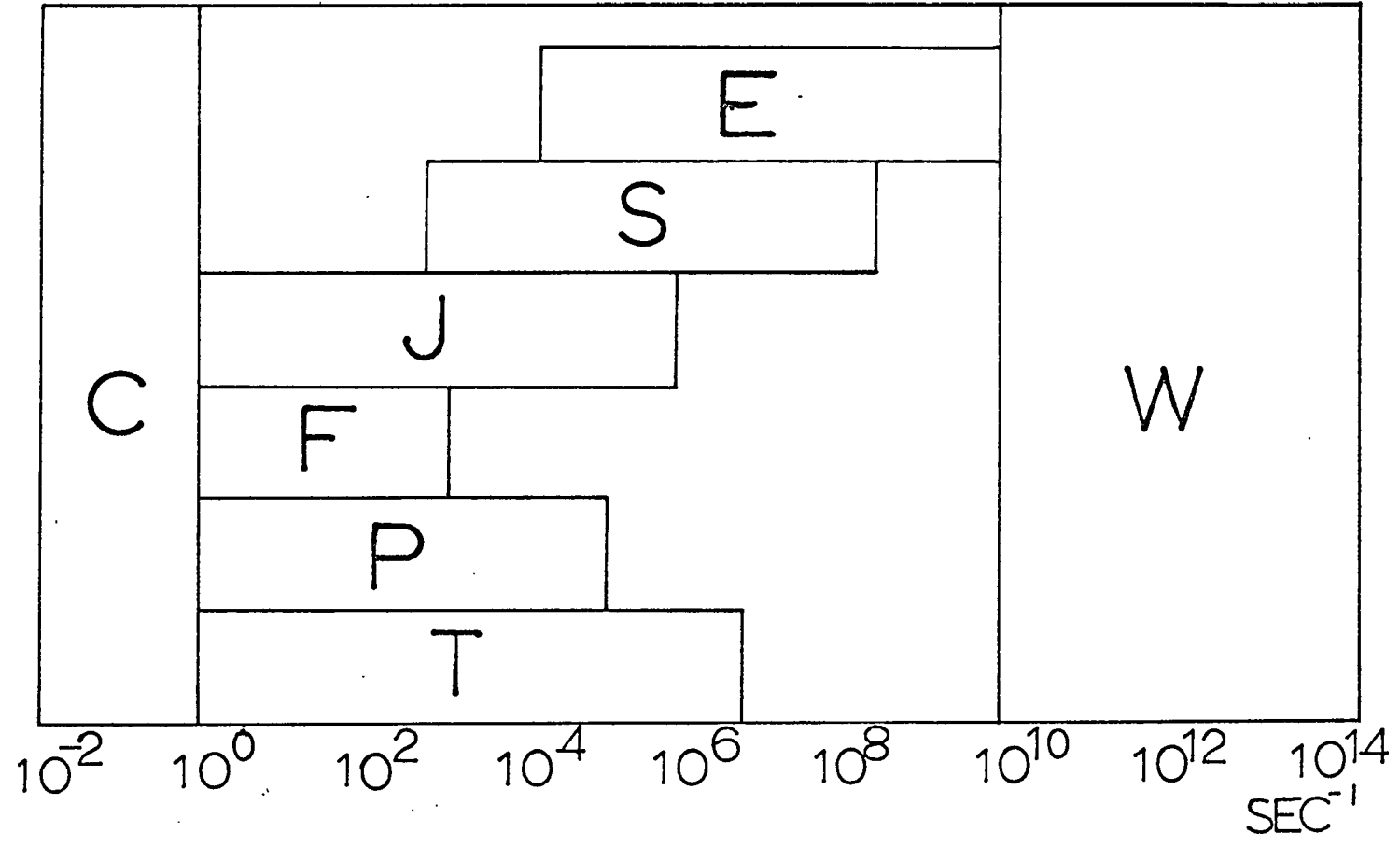
J = Flash

P = Pressure-Jump

T = Temperature-Jump

S = Sound

W = Spectroscopic Range



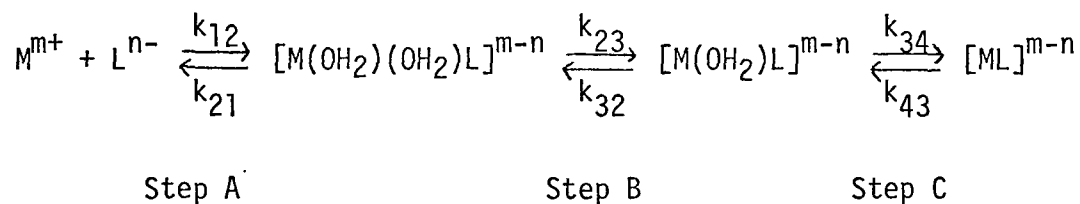
faster than the chemical reactions under investigation. They are unobservable within the time ranges accessible to the relaxation methods and cause no ambiguity in the experimental results.

Most of the experimental data on rates of reactions that occur in the time range from  $10^{-1}$  to  $10^{-10}$  seconds can be explained by two mechanisms (6). For one of these mechanisms, the rate-determining step of complex formation is strongly dependent on the nature of the metal ion, but fairly independent of the entering ligand; however, there is a small effect on the rate constant caused by electrostatic influences of different charge types and steric factors of the ligand. Systematic studies have shown that the divalent ions of the first transition series react by this mechanism. Ions showing strong hydrolysis, such as  $\text{Fe}^{+3}$  and  $\text{Be}^{+2}$  react by the second mechanism. For these ions, the rate is strongly dependent on the basicity of the entering ligand. The distinguishing characteristics of this group is that the rate of hydrolysis exceeds appreciably the possible rate of substitution in the unhydrolyzed complex. Thus a ligand which is a good proton acceptor will accelerate the hydrolysis. Ions like  $\text{Fe}^{+3}$ ,  $\text{Al}^{+3}$  or  $\text{Be}^{+2}$ , show relaxation processes which are quite complicated. Solutions of  $\text{BeSO}_4$  in the pH range of 2-5 exhibit six different relaxation times between 0.1 and  $10^{-9}$  sec (7). Only four of these relaxation times could be interpreted unequivocally. The multiple step mechanism proposed by Eigen (7-9) and his co-workers, shown in Figure 2, will be discussed step by step in Chapter IV.

The rates of ligand substitution reactions involving the nickel(II) ion and different ligands such as oxalate (10) and malonate (11) have been

FIGURE 2

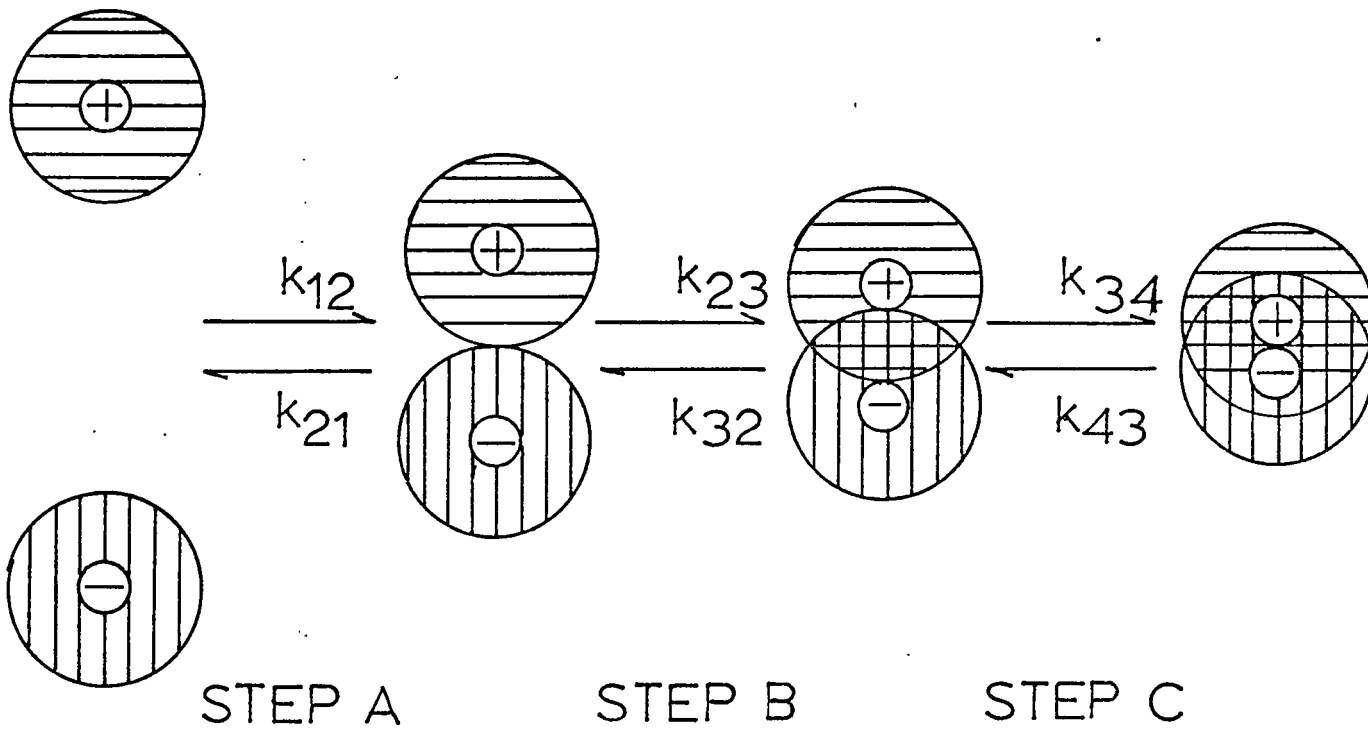
## MULTIPLE STEP COMPLEX FORMATION MECHANISM



Step A = Formation of Bjerrum Ion Pair

Step B = Formation of Outer-Sphere Coordination Complex

Step C = Formation of Inner-Sphere Coordination Complex



reported recently in the literature. In these studies, the rate of oxalate substitution was followed by a flow technique and the rate of malonate substitution followed by a temperature-jump method. The rate constants and the activation parameters for both systems were almost the same indicating that the rate step is independent of the nature of the ligand. In order to determine if a small ligand effect could be found in the rate of ligand substitution for the nickel(II) complexes, the nickel malonate and nickel succinate systems have been studied using a pressure-jump method. By using the same technique on both systems and by carefully evaluating the errors, better comparative results should be obtained which would show if any ligand effect can be detected. The same system has been used to study magnesium oxalate complex in order to compare the rate constant and activation parameters with those of the nickel systems and other magnesium systems reported in the literature (12,13).

## CHAPTER II

### THEORY

## THEORY

A. The Relaxation Time and the Rate Constant

A simplified one-step equilibrium such as complex formation or ion association that is experimentally encountered, can be written as follows:



If the system is initially at equilibrium with the concentrations,  $C_a$ ,  $C_b$ , and  $C_c$ , for the species,  $A^+$ ,  $B^-$ , and  $C$ , respectively, when the equilibrium conditions are suddenly disturbed, the reaction will be shifted to a new equilibrium where the equilibrium concentrations are now  $\bar{C}_a$ ,  $\bar{C}_b$ , and  $\bar{C}_c$ . At time  $t$ , the actual concentrations differ from these by an amount  $x$ , so that,

$$x = C_a - \bar{C}_a = C_b - \bar{C}_b = \bar{C}_c - C_c. \quad (\text{II-2})$$

The net forward rate at time  $t$  is given by

$$-\frac{dx}{dt} = k_f C_a C_b - k_r C_c \quad (\text{II-3})$$

which at equilibrium becomes

$$k_f \bar{C}_a \bar{C}_b - k_r \bar{C}_c = 0. \quad (\text{II-4})$$

The net forward rate is obtained in terms of  $x$  by substituting  $C_a = \bar{C}_a + x$ ,  $C_b = \bar{C}_b + x$  and  $C_c = \bar{C}_c - x$  into equation (II-3). From equation (II-4), the following relationship is obtained by assuming only a small displacement for the reaction

$$-\frac{dx}{dt} = [k_f(\bar{C}_a + \bar{C}_b) + k_r]x \quad (\text{II-5})$$

The quantity in brackets is a constant, independent of time. Integration of equation (II-5) gives

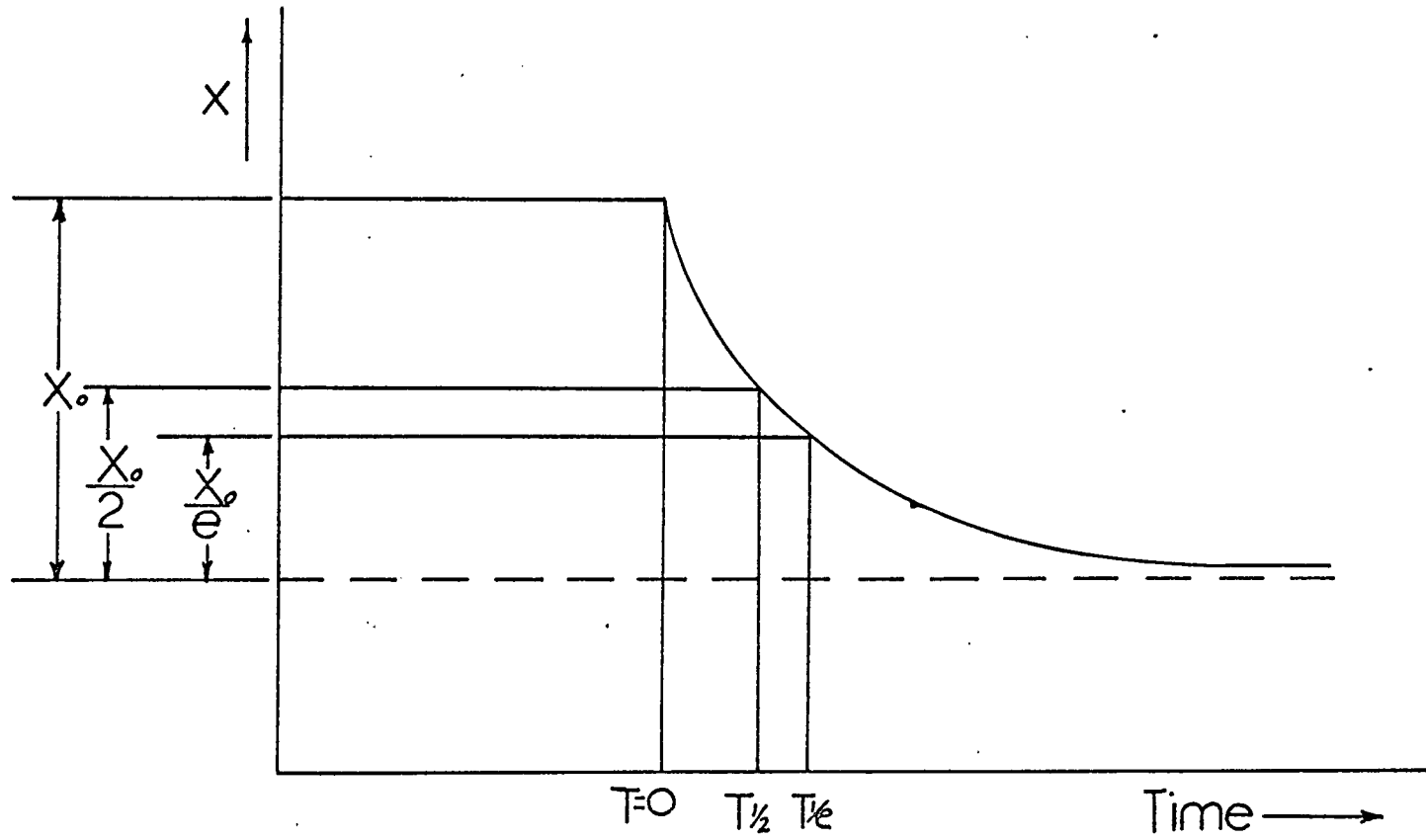
$$\frac{x}{x_0} = e^{-[k_f(\bar{C}_a + \bar{C}_b) + k_r]t} \quad (\text{II-6})$$

where  $x_0$  is the value of  $x$  immediately after the disturbance. Equation (II-6) describes the course of equilibration which is illustrated in Figure 3. It implies that after a time interval such that  $[k_f(\bar{C}_a + \bar{C}_b) + k_r]t = 1$ , then  $\frac{x}{x_0} = \frac{1}{e}$ ; that is, the difference between the actual and equilibrium concentrations has been reduced to  $\frac{1}{e}$  of the original difference. It is convenient to define this time interval as the relaxation time, denoted by  $\tau_1$ . The relaxation time at a series of concentrations can be found experimentally. Therefore, a plot of  $\tau_1^{-1}$  against  $(\bar{C}_a + \bar{C}_b)$  yields a straight line where the slope is the forward rate constant and the intercept is the reverse rate constant as shown below

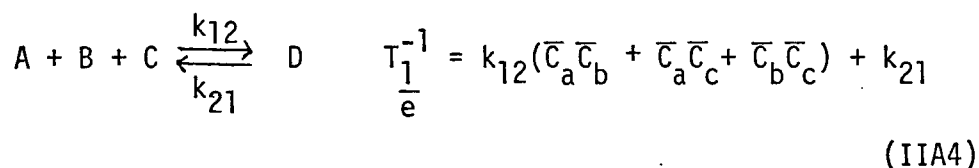
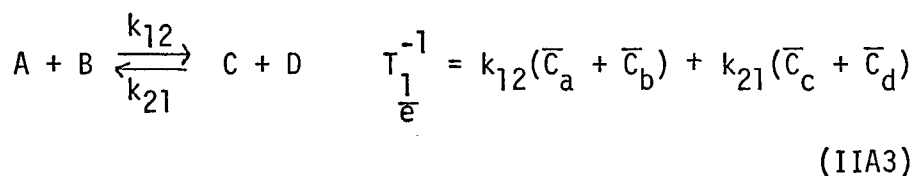
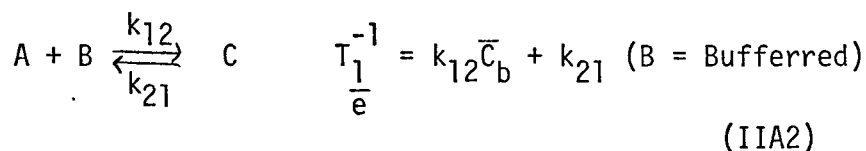
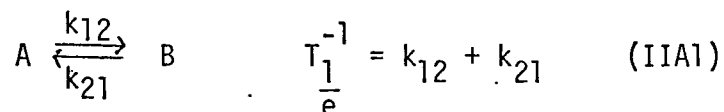
$$\tau_1^{-1} = k_f(\bar{C}_a + \bar{C}_b) + k_r \quad (\text{II-7})$$

FIGURE 3

RELAXATION RESPONSE FOLLOWING A RECTANGULAR STEP FUNCTION



The relationship between the relaxation times and the rate constants for the following reaction system can be derived by a similar procedure as follows:



For ionic reactions, Eigen and his associates (1) have shown that the rate constants usually include concentration dependent terms, as a result of electrostatic interactions with other ions present in the system. The ionic interactions can be described in terms of activity coefficients, which occurs in  $k_f$ , where  $k_r$  remains concentration independent as shown in equation (II-7). Equation (II-7) can now be replaced by

$$T_1^{-1} = k_f^T + k_r \quad (\text{II-8})$$

with

$$k_f^T = k_f f(c). \quad (\text{II-9})$$

The concentration dependent  $f(c)$  is given by

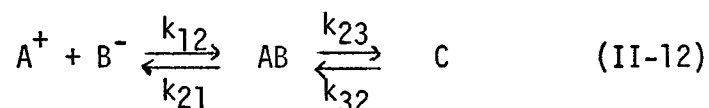
$$f(c) = \frac{1}{\gamma_{\pm}^2} \left\{ C_+ \left( 1 + \frac{\partial \ln \gamma_+}{\partial \ln C_+} \right) + C_- \left( 1 + \frac{\partial \ln \gamma_-}{\partial \ln C_-} \right) \right\} \quad (\text{II-10})$$

where  $C_+$ ,  $C_-$ , and  $\gamma_+$ ,  $\gamma_-$  are the concentrations and activity coefficients of the free ions. The  $\frac{\partial \ln \gamma_i}{\partial \ln c_i}$  terms may be calculated from experimental activity coefficient data after allowance for ion association equilibria or from a theoretical equation based on the Debye-Hückel theory (15).

$$\frac{\partial \ln \gamma_+}{\partial \ln C_+} = \frac{\partial \ln \gamma_-}{\partial \ln C_-} = - \frac{\Gamma z_i^2 C_i^2 (z_+^2 + z_-^2)}{4(1 + \mu^{1/2}) \mu^{1/2}} \quad (\text{II-11})$$

In this equation,  $\Gamma = 0.22$  for water at 25°C and  $\mu$  is the ionic strength of the solution.

In a reaction system,



where the intermediate (e.g., an ion pair) is present at finite concentration and the ionic atmosphere effects (a configurational distri-

bution of ions) are taken under consideration, the linearized rate equations for a small displacement can be written as follows:

$$\frac{dx_1}{dt} = -k_{12}^T x_1 + k_{21} x_2 \quad (\text{II-13})$$

$$\frac{dx_2}{dt} = k_{12}^T x_1 - (k_{21} + k_{23}) x_2 + k_{32} x_3 \quad (\text{II-14})$$

$$\frac{dx_3}{dt} = k_{23} x_2 - k_{32} x_3 \quad (\text{II-15})$$

with  $x_1 = C_a - \bar{C}_a = C_b - \bar{C}_b$ ;  $x_2 = C_{ab} - \bar{C}_{ab}$ ;  $x_3 = C_c - \bar{C}_c$ , and  $k_{12}^T = k_{12}f(c)$ . With the assumption that  $T_1 \ll T_{11}$ , the relaxation times can be solved in the following way:

$$\frac{1}{T_1} = [k_{12}^T + k_{21}] = k_{12}f(c) + k_{21} \quad (\text{II-16})$$

$$\frac{1}{T_{II}} = \{k_{32} + k_{23}k_{12}^T / (k_{12}^T + k_{21})\}$$

$$= \frac{k_{23}f(c)}{f(c) + \frac{k_{21}}{k_{12}}} + k_{32}$$

$$= \frac{K_a k_{23} f(c)}{1 + K_a f(c)} + k_{32} \quad (\text{II-17})$$

where  $K_a$  is the stability constant for the ion pair formation.

Let  $\frac{k_a}{1 + K_a f(c)} k_{23}' = k_{23}'$ , the equation (II-17) is reduced to

$$\frac{1}{T_{II}} = k_{23}' f(c) + k_{32} \quad (\text{II-18})$$

where  $T_I$  and  $T_{II}$  refer to the relaxation times corresponding to step I and step II respectively.

A generalized equation thus can be derived for the mechanism shown in Figure 2.

$$\frac{1}{T_i} = k_{k1}' [f(c)] + k_{1k} \quad (\text{II-19})$$

where  $k_{k1}'$  are the effective rate constants defined specifically by:

$$k_{12}' = k_{12} \quad (\text{II-20})$$

$$k_{23}' = \frac{k_a}{1 + K_a [f(c)]} k_{23} \quad (\text{II-21})$$

$$k_{34}' = \frac{K_a K_b}{1 + K_a (1 + K_b) [f(c)]} k_{34} \quad (\text{II-22})$$

$K_a$  and  $K_b$  are the stability constants for step a and b, respectively, and  $k_{34}$ ,  $k_{43}$  are much smaller than  $k_{12}$ ,  $k_{21}$  or  $k_{23}$ ,  $k_{32}$ .

The above treatment shows that the observed rate constants for each step not only depend on the ionic interactions but also concentrations of the free ions and the stability constants for the ion pair formation.

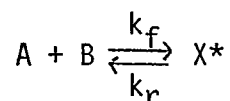
Thus, only in very dilute solutions and with complexes with a small

stability constants can  $k_{k1}$  be treated as a constant, otherwise the plot of concentrations of the free ions against the reciprocal of the relaxation times will not give a straight line.

Also, it should be noted that the separation of the individual relaxation times in a given relaxation oscillogram may have considerable experimental difficulties if their relaxation times differ by less than an order of magnitude since they are not easily separated from this pattern.

#### B. Kinetics of Fast Reactions in Solution

The equilibrium constant for the process



may be written as

$$\frac{RT}{Nh} k^* = k \quad (II-23)$$

since  $RT \ln k^* = -\Delta G^*$ , equation (II-23) can be rewritten as

$$k = \frac{RT}{Nh} e^{-\frac{\Delta G^*}{RT}} \quad (II-24)$$

where  $\Delta G^*$  is the increase in Gibbs free energy in the passage from the initial state to the activated state, R, the gas constant, N, Avogadro's number, h, Planck's constant, and k, either the forward or reverse rate constant.

This free energy of activation,  $\Delta G^*$ , can be expressed in terms of an entropy and a heat of activation in the following way

$$k = \frac{RT}{Nh} e^{-\frac{\Delta H^*}{RT}} e^{\frac{\Delta S^*}{R}}, \quad (\text{II-25})$$

The variation of  $k^*$  with temperature is given by

$$\frac{d \ln k^*}{dT} = \frac{\Delta E^*}{RT^2} \quad (\text{II-26})$$

where  $\Delta E^*$  is the increase in energy in passing from the initial state to the activated state. Differentiation of the logarithmic form of equation (II-23) and substitution into equation (II-26) result in

$$\frac{d \ln k}{dT} = \frac{1}{T} + \frac{\Delta E^*}{RT^2} = \frac{RT + \Delta E^*}{RT^2}. \quad (\text{II-27})$$

Equating this equation to the Arrhenius equation gives

$$\frac{d \ln k}{dT} = \frac{\Delta E_{\text{exp}}}{RT^2} = \frac{RT + \Delta E^*}{RT^2} \text{ and} \quad (\text{II-28})$$

$$\Delta E_{\text{exp}} = RT + \Delta E^*$$

The relationship between  $\Delta E^*$  and  $\Delta H^*$ , and  $\Delta H^*$  and  $\Delta E_{\text{exp}}$  is,

$$\Delta H^* = \Delta E^* + P\Delta V^* \quad (\text{II-29})$$

$$\Delta H^* = \Delta E_{\text{exp}} + P\Delta V^* - RT \quad (\text{II-30})$$

since  $\Delta V^*$  is small for reaction in solution

$$\Delta H^* = \Delta E_{\text{exp}} - RT \quad (\text{II-31})$$

Again equate the Arrhenius equation to equation (II-25), we have

$$\ln k = \ln A - \frac{\Delta E_{\text{exp}}}{RT} = \ln \frac{RT}{Nh} - \frac{\Delta H^*}{RT} + \frac{\Delta S^*}{R} \quad (\text{II-32})$$

Substituting equation (II-31) into equation (II-32) gives

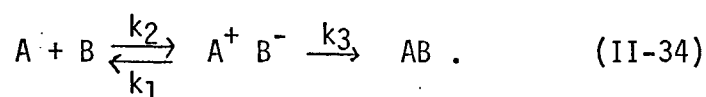
$$\ln A = \ln \frac{eRT}{Nh} + \frac{\Delta S^*}{R} \quad (\text{II-33})$$

Using equations (II-32) and (II-33), a plot of the logarithmic rate constants against the reciprocal of the temperatures gives the experimental activation energy and also  $\ln A$ . Thus, the best values of enthalpy of activation, entropy of activation and free energy of activation which determines the kinetic lability of the reaction are obtained.

Most reactions with activation energies around  $10 \text{ kcal/mole}^{-1}$  proceed very fast with a frequency factor,  $A$ , of  $10^{11} \text{ mole}^{-1} \text{ sec}^{-1}$ , (a representative value for many reactions between anion and a molecule) (16), a change in activation energy from  $14 \text{ kcal/mole}^{-1}$  to  $4 \text{ kcal/mole}^{-1}$

will have corresponding change in the second-order rate constant from  $10 \text{ molar}^{-1}\text{sec}^{-1}$  to  $10^8 \text{ molar}^{-1}\text{sec}^{-1}$ . For the fastest reactions ( $E_a < 4 \text{ kcal/mole}^{-1}$  in this case), the validity of the Arrhenius equation breaks down and the rate for these reactions can be calculated from the diffusion theory.

Consider the complex formation reaction



With the aid of the steady state assumption, the observed forward rate constant can be obtained from the following rate expression

$$\frac{d(AB)}{dt} = -\frac{dA}{dt} = -\frac{dB}{dt} = \frac{k_2 k_3}{k_1 + k_3} [A][B] \quad (\text{II-35})$$

$$\text{then } k_f = \frac{k_2 k_3}{k_1 + k_3} \quad (\text{II-36})$$

If the complex is much more likely to react than to revert (i.e. if  $k_3 \gg k_1$ ), then  $k_f = k_2$ ; the mechanistic equivalent to this assumption is that the activation energy of the reaction is equal to the activation energy ( $E_2$ ) controlling  $k_2$  which makes the rate-determining step for this system the first step. Reaction (II-34) actually corresponds to the last and slowest step of the substitution mechanism shown in Figure 2. Since the rate of direct combination of the ligand and the metal ion is much faster than the dissociation of the water molecule, it is logical to

combine these two steps into one. In the case of polydentate complex formation, the same argument can be applied by considering one more step which will be proved later in the discussion.

### C. Nature of the Pressure-Jump Method

The pressure-jump method, using conductivity measurements to follow the relaxation process in the study of dissociation processes in electrolytic solutions, offers some advantages over the temperature-jump technique which has to use optical methods to follow the relaxation processes. The conductivity is a direct function of the free ion concentration and, therefore, is a direct measurement of the extent of dissociation. Thus, possible complications associated with the introduction of the indicator systems used with the temperature-jump technique are avoided.

The biggest disadvantage found in the pressure-jump method is that the minimum relaxation time is limited by the rectangular step-forced function which has a finite risetime; in this case it is the time required for the applied high pressure to be restored to room atmospheric pressure. In other words, the range of measurable rate constants is limited. Also, when the measured relaxation times are close to the rise time, they become very sensitive to the acoustical transients occurring with the cell assembly resulting from the disturbance of the releasing pressure.

The magnitude and concentration dependence of the relative change in the specific conductance ( $\frac{\delta \kappa}{\kappa}$ ) for a weak and dilute electrolyte solution with a pressure change can be treated as follows:

$$\kappa = \frac{F}{1000} \sum_n C_n |Z_n| \mu_n = \frac{F\rho}{1000} \sum_n M_n |Z_n| \mu_n$$

(II-38)

where  $\kappa$  is specific conductance (in  $\text{ohm}^{-1} \text{cm}^{-1}$ ),  $\mu$  is the mobility, and  $C_n$  and  $M_n$  are the molar and molal concentration, respectively, of the  $n^{\text{th}}$  type of ion,  $\rho$  is the density, and  $F$  the Faraday constant. The change in specific conductance brought about by an effect of perturbation of the system on the concentrations, density and mobilities is given by neglecting second-order terms

$$\delta\kappa = \frac{F}{1000} \left[ \sum_n |Z_n| \mu_n \delta C_n + \sum_n |Z_n| C_n \delta \mu_n + \sum_n |Z_n| \mu_n M_n \delta \rho \right]$$

(II-39)

Change in conductivity due to changes in concentrations, mobilities of the ions, and volume of the solution is represented by the first, second, and third terms in equation (II-39), respectively. It, therefore, represents the chemical relaxation process. The effects of changes on mobilities and the volume follow the pressure change almost instantaneously and are cancelled from the measurements by a differential technique. Hence, for the chemical contribution to the change in conductivity, one may write simply

$$\frac{\delta\kappa}{\kappa} = \frac{\sum_i |Z_i| \mu_i \delta C_i + \sum_j |Z_j| \mu_j \delta C_j}{\sum_n |Z_n| \mu_n C_n}$$

(II-40)

where the denominator includes the contributions to the total conductivity from all ionic species present in the solution and the numerator reflects only those ionic components involved in pressure sensitive equilibria, (i refers to reactants, j products). For strong electrolytes with little ion association,  $\frac{\delta \kappa}{\kappa}$  is relatively independent of concentration for a given pressure change.

Since a rapid pressure change takes place essentially adiabatically, a temperature change accompanying the pressure step will affect the concentration changes also. For instance, a 30-atm pressure step is accompanied by a temperature change of about 0.05°C for aqueous solutions at 25°C. Usually the conductivity change due to this temperature change is small compared to that brought about by the pressure change. However, the fact that the system has been perturbed by an adiabatic pressure change rather than an isothermal change does not influence the determination of the relaxation time, since the temperature was raised in both cells at the same time.

The relaxation time is determined by  $k_r$  and  $k_f (\bar{C}_a + \bar{C}_b)$  as shown in equation (II-7). Before  $k_f$  and  $k_r$  can be determined, conditions must be found which will make the relaxation time concentration dependent. This can be done by picking a system that has a small enough  $k_r$  and by controlling the concentrations. Even though the value of  $k_f (\bar{C}_a + \bar{C}_b)$  can be diminished by diluting the solution, the forward rate constant still cannot be measured for most reactions with second-order rate constants larger than  $10^7 - 10^8 \text{ mole}^{-1} \text{ sec}^{-1}$  because the sensitivity of the apparatus becomes abnormally low for a very dilute solution. The same is also true for a strong ionic strength solution. The low sensitivity

is due in this case to the small change in  $\delta\lambda$  or  $\frac{\delta\lambda}{\lambda}$  as illustrated in equation (II-39) or equation (II-40). For these reasons only certain systems can be studied by the pressure-jump method.

CHAPTER III  
EXPERIMENTAL

## EXPERIMENTAL

A. Apparatus

The apparatus (Figure 4) constructed in this laboratory is similar to that described by Strehlow and Becker (3). The apparatus consists of three principal parts: The first part is to initiate the stepwise disturbance, another part is to detect some change in the reaction caused by the disturbance, and the third part is to record the change between the two different equilibrium conditions.

A pressure of about 20 to 30 atmospheres is applied to a dual conductivity cell arrangement in order to establish an equilibrium at a higher pressure. The air pressure in the cavity is transmitted directly to the two conductivity cells through the diaphragms and pressure sensitive tape, these serve to separate the solutions from the air space above and contain the liquid when the pressure is suddenly released. After the sudden pressure decrease by the burst of the brass diaphragm, the relaxation effects are followed by means of a Wheatstone bridge (Figure 5) with the two cells in separate arms of the bridge.

A general radio sine wave generator was used to provide a 200 kc signal across the conductivity bridge. Since an ungrounded source was used to drive the bridge, it was necessary to introduce a shielded transform (General Radio, 578-C) to couple the bridge with the generator.

The A.C. signal was displayed on a dual gun cathode ray oscilloscope (Tektronix, Model 547) with an amplifier (Tektronix, Type D). The oscilloscope was triggered internally by means of a rectified signal. It was necessary to insure that the oscilloscope triggered as closely to

FIGURE 4  
THE PRESSURE-JUMP APPARATUS

- A = Steel Plunger
- B = Muffler
- C = Copper-Beryllium Foil
- D = Diaphragms
- E = Pressure Capillary
- F = Conductivity Cells
- G = Copper Coil
- H = Electrodes

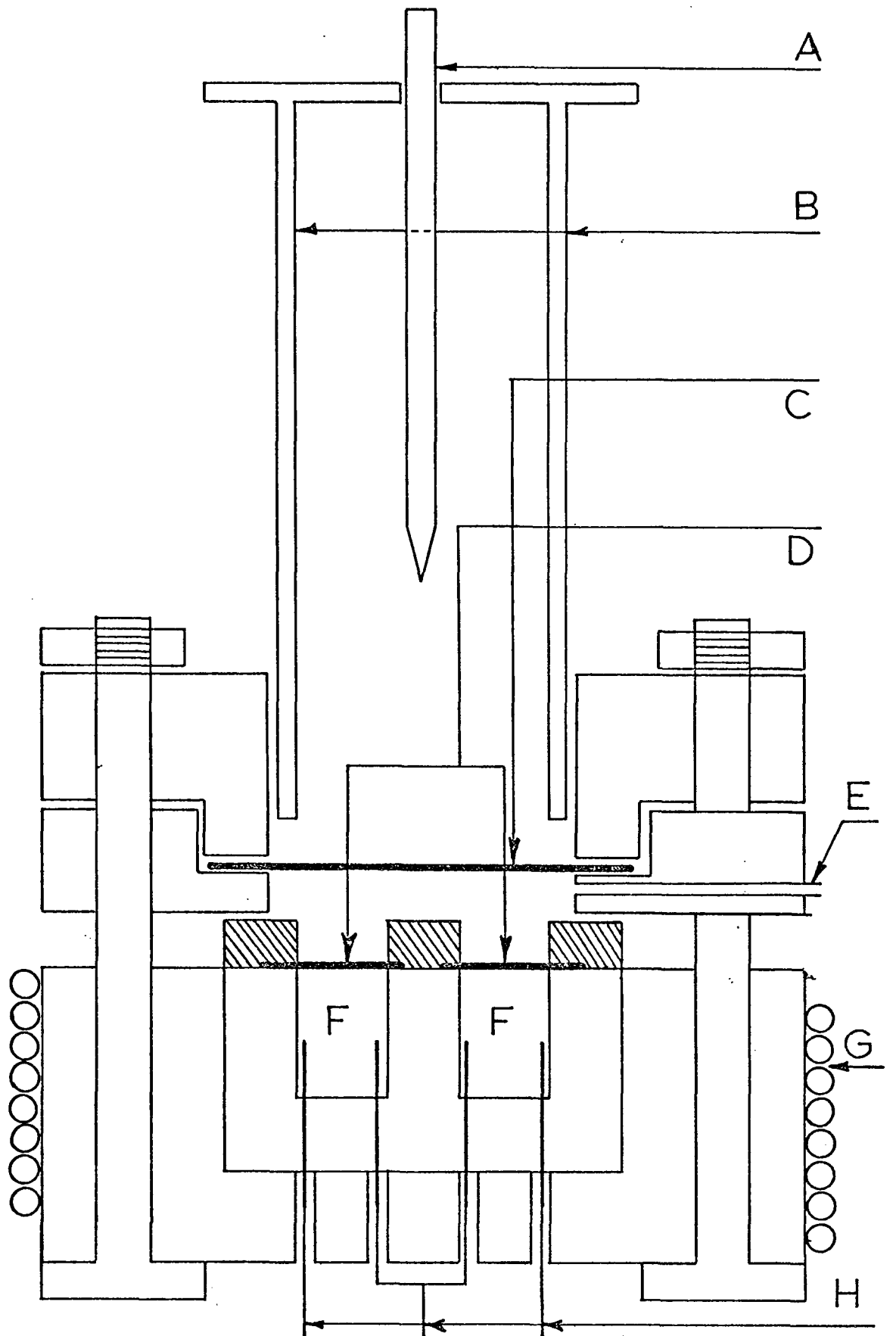


FIGURE 5  
THE CONDUCTIVITY CELL

C = Cells

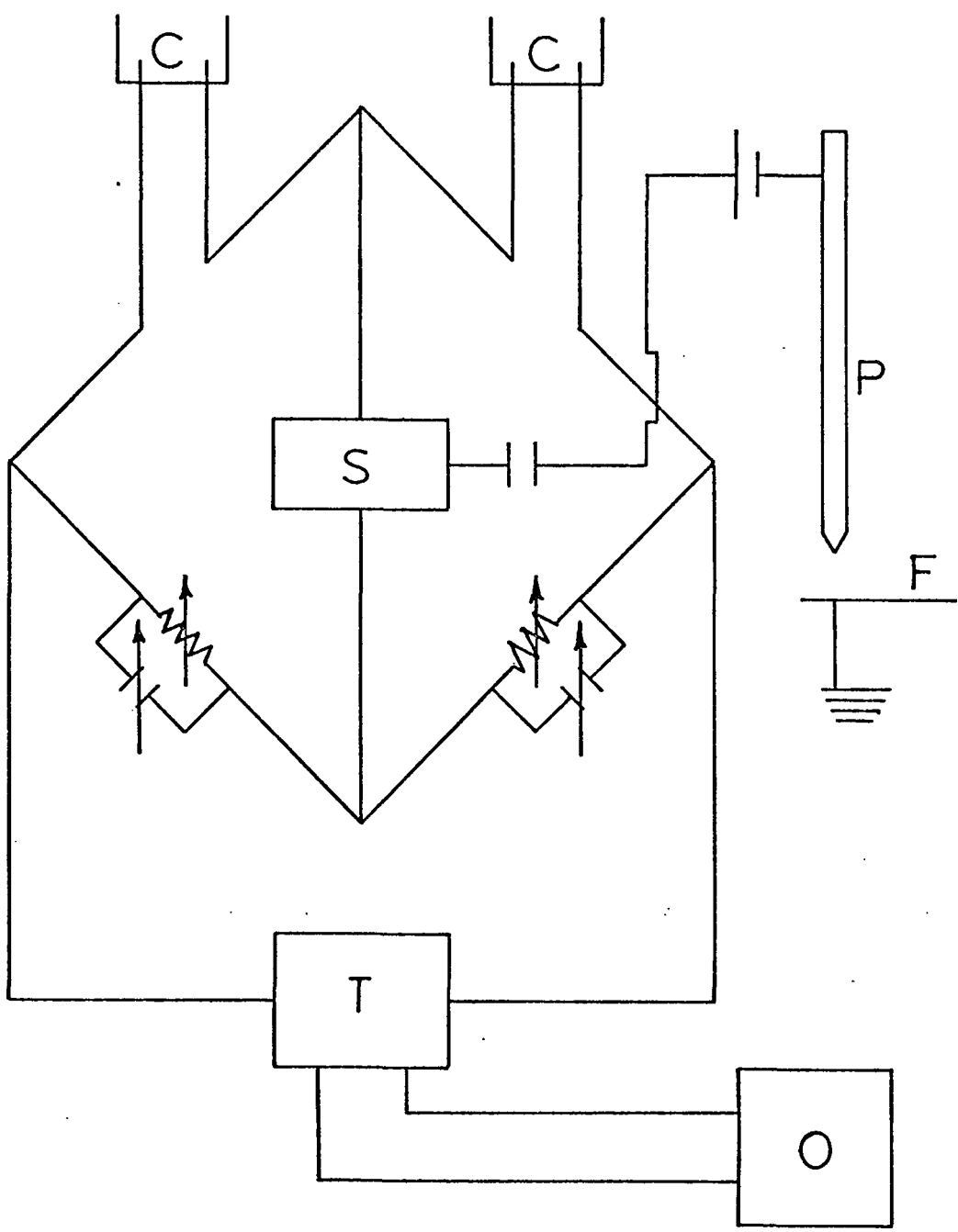
F = Foil

O = Oscillator

P = Plunger

S = Scope

T = Transformer



zero time as possible. The course of re-equilibration was photographed by a polaroid camera mounted on the oscilloscope. One of the two cells was filled with the solution to be studied, the other with solution of a different electrolyte with a similar conductivity. The conductivity should be the same in order to avoid overloading the detector circuits. Each solution was thoroughly degassed to reduce cavitation effects associated with the development of a tension wave resulting from the rapid pressure release. The relaxation time of the reference electrolyte, potassium chloride, used in this experiment was shorter than one microsecond so it had no influence on the relaxation process of the solution studied. The use of this difference technique, which allows compensation of the density and mobility effects as described above, leads to greater sensitivity and precision of the measurements.

When the time interval of the step-forcing function (release of pressure) is of the same order of magnitude as the relaxation time being measured, it is necessary to correct the observed value by use of the following equation

$$\frac{1}{e} = \left[ \frac{1}{(T_i - T_s)} \right] \left[ T_i e^{-\frac{t}{T_i}} - T_s e^{-\frac{t}{T_s}} \right] \quad (\text{III-1})$$

where  $T_s = 77 \pm 10$  microseconds in this case and  $t$  refers to the measured relaxation time which is a combination of the perturbing function and the chemical relaxation.

The relaxation process (step-forcing function) due to the pressure decrease can be measured by the study of 0.2 M  $\text{NiSO}_4$  since this solution has a relaxation time shorter than two microseconds (Figure 6). Typical

examples of the chemical relaxation process for nickel(II) malonate, nickel(II) succinate, and magnesium oxalate, are shown in (Figures 7-10). As can be seen from these curves, the best results were obtained when the relaxation times were longer than 0.5 microseconds. This is because of the acoustical produced signals picked up when fast sweep rates are used.

The relaxation time is measured as shown in (Figure 11). The quantities A and B are proportional to the equilibrium concentrations in the cell at two different sets of conditions. The difference between A and B is equal to  $2x_0$ . C is obtained by adding  $\frac{2x_0}{e}$  to B, where the term  $\frac{2x_0}{e}$  corresponds to the concentration difference which is reduced to  $\frac{1}{e}$  of the original deviation,  $2x_0$ . Then the relaxation time,  $T_{\frac{1}{e}}$ , can be measured directly from the oscillogram.

#### B. Preparation of the Solutions

Nickel malonate and nickel succinate were prepared by mixing stoichiometric amounts of nickel sulfate with the acid and then titrating with a standard solution of barium hydroxide until all the sulfate ion had precipitated as barium sulfate. The solid barium sulfate was removed by filtration and the resulting solution of the pure nickel salt to be studied was diluted to the desired concentrations. The pH of the solution ranged from 7.5 to 7.9 and 7.4 to 7.8 for the nickel malonate and the nickel succinate, respectively. Since the  $pK_1$  and  $pK_2$  of the malonic acid and succinic acid are 2.85, 6.10 and 4.19, 5.57 respectively, most of the ligand molecules are present in the anionic form.

## FIGURE 6

PRESSURE-JUMP (WITHOUT CHEMICAL RELAXATION PROCESS)

$[\text{NiSO}_4] = 0.2 \text{ M}$ , Sweep Rate =  $0.1 \text{ m sec/cm}$

The Risetime of the Apparatus =  $52 \mu\text{sec}$

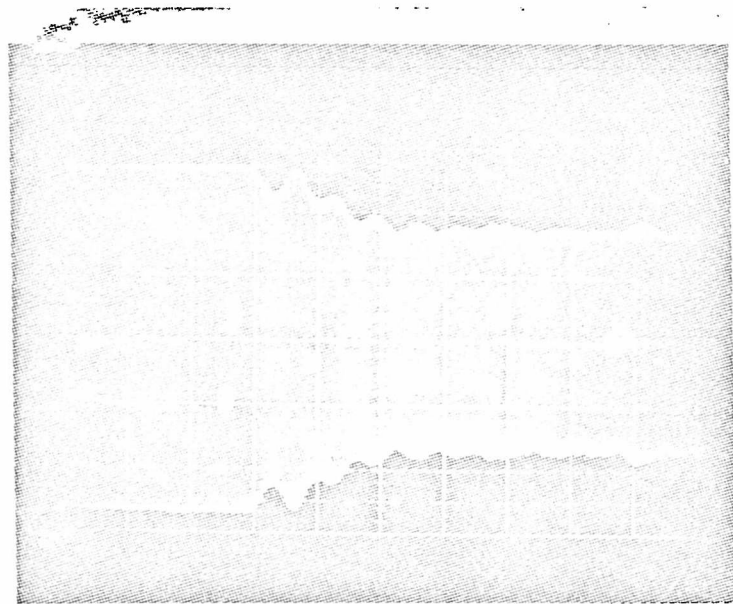


## FIGURE 7

## EXPERIMENTAL RELAXATION CURVE FOR NICKEL MALONATE

Temp = 23.5°C, PH = 7.95,  $\mu = 3.73 \times 10^{-3}$  M

[NiMal] =  $8.0 \times 10^{-3}$  M. Sweep Rate = 2 m sec/cm

Measured Relaxation Time =  $2.5 \times 10^{-3}$  sec

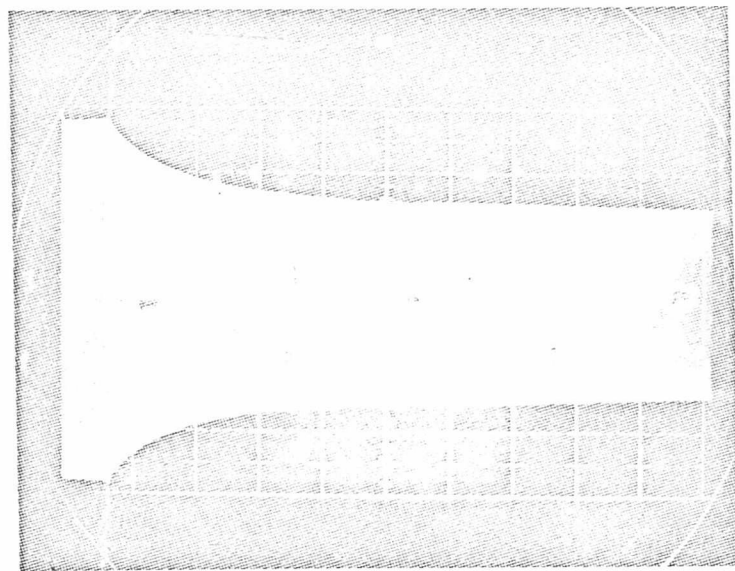


## FIGURE 8

## EXPERIMENTAL RELAXATION CURVE FOR NICKEL MALONATE

Temp = 32.5°C, PH = 7.95,  $\mu = 3.73 \times 10^{-3}$  M

[NiMal] =  $8.0 \times 10^{-3}$  M. Sweep Rate = 1 m sec/cm

Measured Relaxation Time = 1.33 m sec

Chemical process Relaxation Time = 1.25 m sec

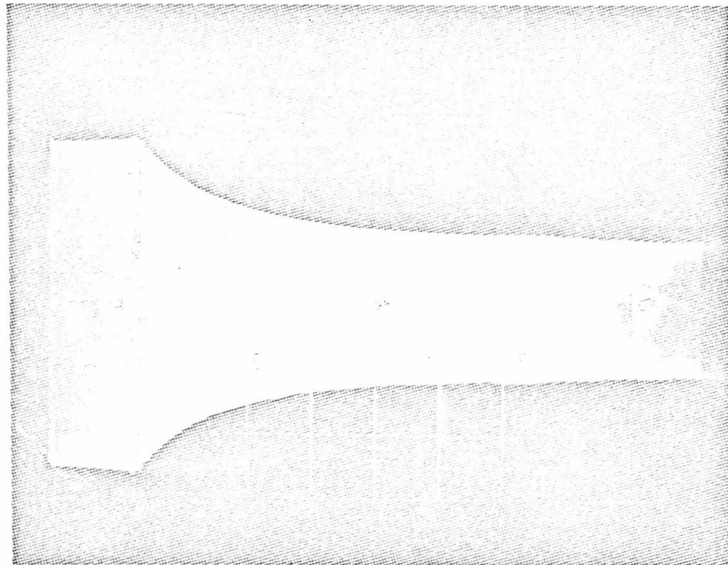


## FIGURE 9

## EXPERIMENTAL RELAXATION CURVE FOR NICKEL SUCCINATE

Temp = 16.8°C, PH = 7.8,  $\mu = 3.79 \times 10^{-3}$  M

[NiSucc] =  $6.7 \times 10^{-3}$  M. Sweep Rate = 0.5 m sec/cm

Measured Relaxation Time = 414  $\mu$ sec

Chemical Process Relaxation Time = 328  $\mu$ sec

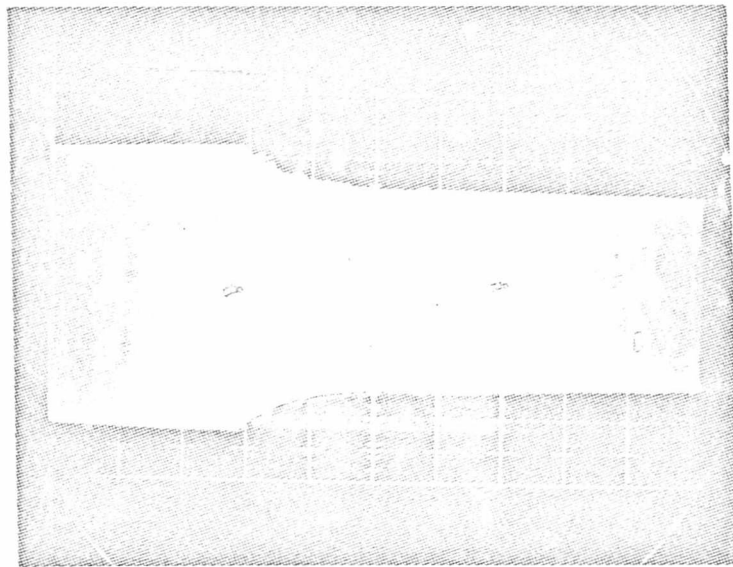


## FIGURE 10

## EXPERIMENTAL RELAXATION CURVE FOR MAGNESIUM OXALATE

Temp = 23.5°C, PH = 7.0, [MgOX] =  $1.0 \times 10^{-3}$  M

Sweep Rate = 0.2 m sec/cm

Measured Relaxation Time = 228  $\mu$ sec

Chemical Process Relaxation Time = 140  $\mu$ sec

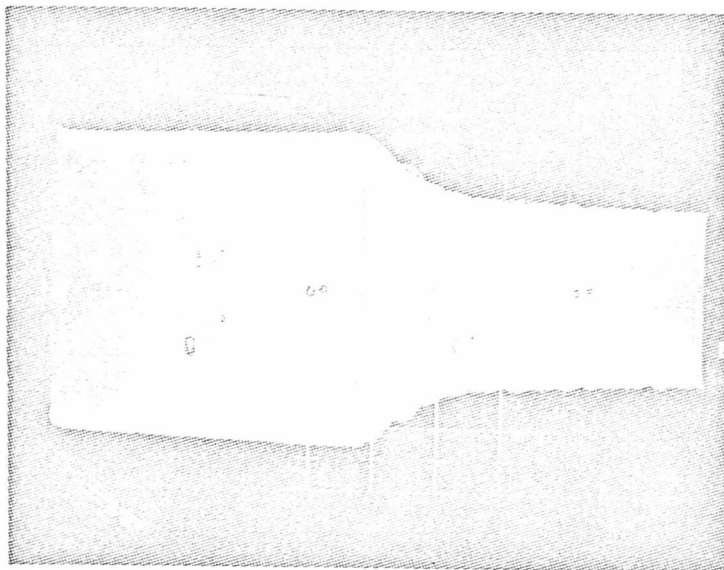
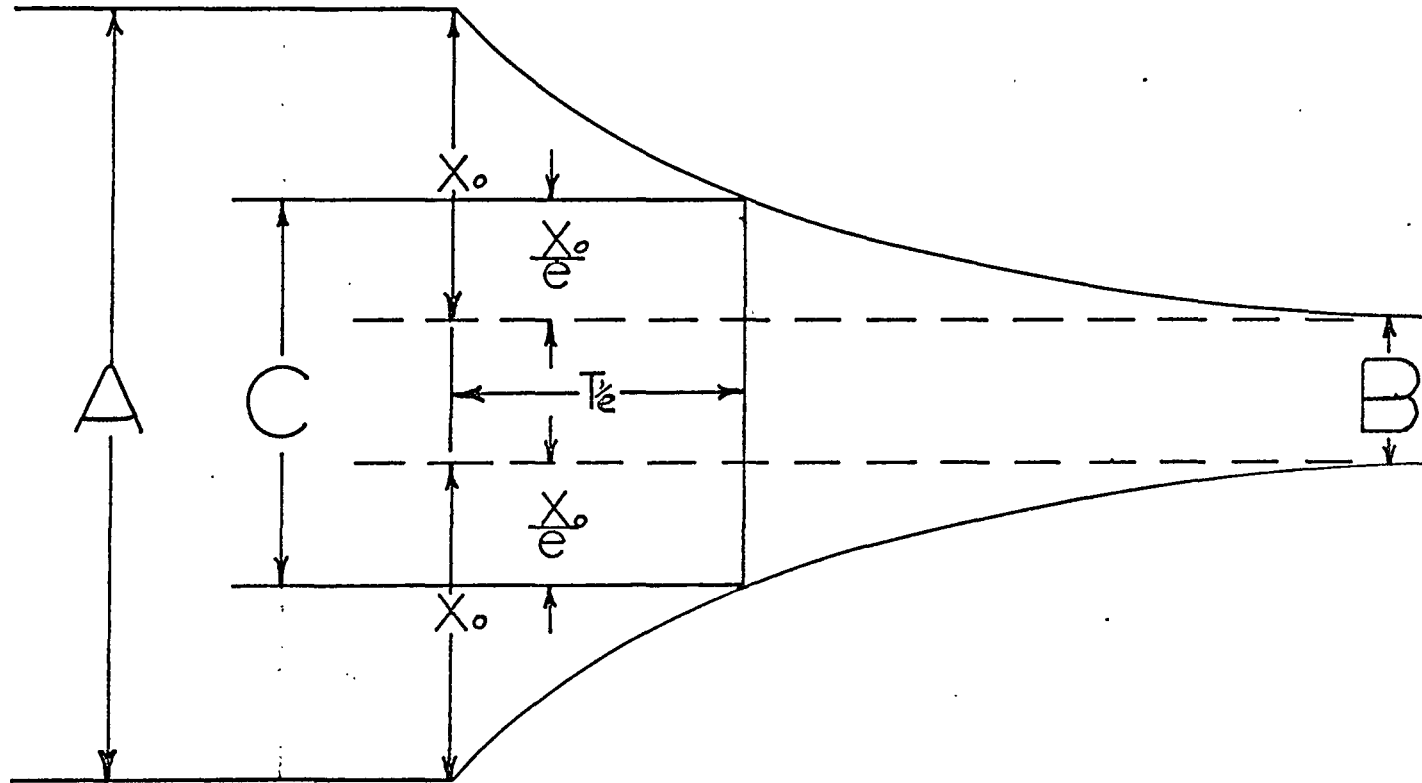


FIGURE 11  
MEASUREMENT OF THE RELAXATION TIME  
FROM THE OSCILLOGRAM PATTERN



The  $\text{MgC}_2\text{O}_4 \cdot 2\text{H}_2\text{O}$  was prepared (17) from aqueous solutions of equal volume of 0.5 M  $\text{MgCl}_2$  and 0.55 M  $\text{Na}_2\text{C}_2\text{O}_4$ . The former was added rapidly to the latter after both solutions were brought to the boiling point. The mixture was stirred continuously as it was cooled back to room temperature. The fine crystals of the  $\text{MgC}_2\text{O}_4 \cdot 2\text{H}_2\text{O}$  formed were filtered and washed several times with distilled water, dried and stored over magnesium perchlorate in desiccator.

The magnesium oxalate solutions were analyzed by titration with standard EDTA solution.(18). The pH values of the magnesium oxalate solutions ranged from 6.2 to 7.0. Since under these conditions there is danger of forming hydroxy species of the cation, relaxation times at a constant overall concentration were measured as a function of pH. The observation of a pH-independent relaxation times was taken to indicate that the observed relaxation effect was due to ion association between the cation and the ligand and not to hydrolysis of the cation.

Measurements were made at 14.5°C, 23.5°C and 32.5°C for the nickel malonate system, 12.5°C, 17°C and 21.5°C for the nickel succinate system, and 12.8°C, 18.5°C and 23.5°C for the magnesium oxalate system. The lower temperature used for the nickel succinate system and magnesium oxalate system was necessary due to the large value of  $k_r$ .

The relaxation time was determined for different concentrations at each temperature. All of the solutions exhibited a relaxation time which was characterized by a single relaxation step. The concentration of nickel ion, magnesium ion, acid anion, and complexes for each solution was calculated from stability constant data (19,20,21). In all cases the

concentrations were corrected for changes in activities according to the following semi-empirical equation given by Davies (22)

$$\log \gamma_i = - \frac{1}{2} z_i^2 \left[ \frac{\mu^{1/2}}{1 + \mu^{1/2}} - 0.3\mu \right] \quad (\text{III-2})$$

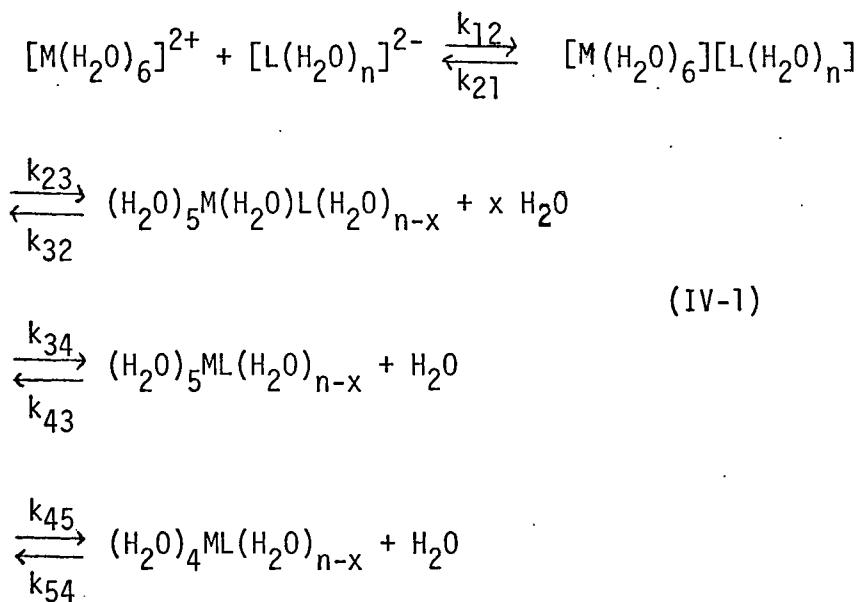
where  $\gamma_i$  is the activity coefficient and  $z_i$  is the charge of the  $i^{\text{th}}$  ion, and  $\mu$  is the ionic strength of the solution. This equation has been found to give activity coefficients reliable to  $\pm 2\%$  up to ionic strength 0.1  $M_0$  for virtually all electrolytes to which it has been applied.

From the desired ionic concentration of the cation and anion, activity coefficients were obtained from equation (III-2). The concentration of the salts were evaluated from the value of the overall stability constant at infinite dilution. The quantity,  $\frac{\partial \ln r_i}{\partial \ln c_i}$ , was found to be negligible on the basis of equation (II-10) for concentrations less than  $C_0 = 0.04M$ .

CHAPTER IV  
RESULTS AND DISCUSSIONS

## RESULTS AND DISCUSSION

The generally accepted mechanism for complex formations between the metal ion and a bidentate ligand,  $L^{-2}$ , is a multiple step system proposed by Eigen and his co-workers (7,9,23). This mechanism is represented by the equations:



where  $M^{+2}$  represents either nickel(II) or magnesium(II), and  $L^{-2}$  either malonate ion, succinate ion or oxalate ion.

The first step in the process is the diffusion controlled approach of the two hydrated ions to form an ion-associate in which the ions are separated by the strongly bonded water molecules of the inner hydration sphere. The second step, believed to involve the loss of a water molecule between the ions which was originally associated with the anion, is generally held to occur less rapidly. The third step, usually found to be the slowest and rate determining, involves the loss of a water molecule

from the inner hydration sphere of the metal ion and the formation of the metal ligand bond. The final step is the formation of the second metal ligand bond to form the fully chelated species.

An evaluation of the rate constants for the third step (formation of inner sphere complex) can be obtained by using equations (II-10) and (II-22).

The rate of formation of the metal monodentate complex can be expressed by

$$\frac{d[ML(aq)]}{dt} = k_{34}[M(aq)L] - k_{43}[ML(aq)], \quad (IV-2)$$

With the assumption of a steady state system, this equation becomes

$$\frac{d[ML(aq)]}{dt} = K_a K_b k_{34} [M^{+2}][L^{-2}] - k_{43}[ML(aq)] \quad (IV-3)$$

The forward rate constant,  $k_f$ , then is given by

$$k_f = k_{34} K_a K_b = k_{34} [1 + K_a(1 + K_b)f(c)] \quad (IV-4)$$

and the reverse rate constant,  $k_r$ , is  $k_{43}$ .

The forward rate constant,  $k_f$ , can be expressed in terms of the measured relaxation time,  $k_a$ ,  $k_b$ ,  $k_{eq}$ , and  $f(c)$  in the following way

$$k_f = \frac{1}{T} \frac{K_{eq}[1 + K_a(1 + K_b)f(c)]}{f(c)[K_{eq} + K_a + K_a K_b] + 1} \quad (IV-5)$$

TABLE I  
RELAXATION TIMES AND  $f(c)$  FOR NICKEL(II) MALONATE AT 14.5°C ( $\mu \rightarrow 0$ )

$C_0$ (M)	$T \times 10^3$ (sec)	$\gamma_{\pm}$	$f(c) \times 10^4$ (M)	pH	Electrolyte(KCl) ( $M \times 10^3$ )
$1.6 \times 10^{-3}$	10.34	0.84	6	7.5	0.83
$1.6 \times 10^{-3}$	10.32	0.84	6	7.5	0.83
$8.0 \times 10^{-3}$	5.0	0.75	13.5	7.95	2.2
$8.0 \times 10^{-3}$	5.28	0.75	13.5	7.95	2.2
0.02	2.64	0.696	19.5	7.8	3.8
0.02	2.69	0.696	19.5	7.8	3.8
0.04	2.03	0.654	26.1	7.9	6
0.04	2.12	0.654	26.1	7.9	6

TABLE II  
RELAXATION TIMES AND F(c) FOR NICKEL(II) MALONATE AT 23.5°C ( $\mu \rightarrow 0$ )

$C_0(M)$	$T_0 \times 10^3(sec)$	$T \times 10^3(sec)$	$\gamma_{\pm}$	$f(c) \times 10^4(M)$
$1.6 \times 10^{-3}$	4.62	4.62	0.86	5.5
$1.6 \times 10^{-3}$	4.62	4.62	0.86	5.5
$8 \times 10^{-3}$	2.5	2.5	0.77	11.6
$8 \times 10^{-3}$	2.69	2.69	0.77	11.6
0.02	1.60	1.60	0.72	17.2
0.02	1.60	1.60	0.72	17.2
0.04	1.19	1.11	0.67	23.4
0.04	1.18	1.10	0.67	23.4

$T_0$  = Measured relaxation times

T = Chemical process relaxation times

TABLE III  
RELAXATION TIMES AND  $f(c)$  FOR NICKEL(II) MALONATE AT 32.5°C ( $\mu \rightarrow 0$ )

$C_0(M)$	$T_0 \times 10^3(sec)$	$T \times 10^3(sec)$	$\gamma_{\pm}$	$f(c) \times 10^4(M)$
$1.6 \times 10^{-3}$	2.4	2.4	0.85	5
$1.6 \times 10^{-3}$	2.3	2.3	0.85	5
$8 \times 10^{-3}$	1.33	1.25	0.77	11
$8 \times 10^{-3}$	1.31	1.23	0.77	11
0.02	0.83	0.75	0.72	16.5
0.02	0.89	0.77	0.72	16.5
0.04	0.63	0.55	0.67	22.2

$T_0$  = Measured relaxation times

$T$  = Chemical process relaxation times

TABLE IV  
RELAXATION TIMES AND F(c) FOR NICKEL(II) SUCCINATE AT 12.5°C ( $\mu \rightarrow 0$ )

$C_0$ (M)	$T_0 \times 10^3$ (sec)	$T \times 10^3$ (sec)	$\gamma_{\pm}$	$f(c) \times 10^4$ (M)	pH
$3.74 \times 10^{-3}$	576	492	0.645	25.9	7.5
$3.74 \times 10^{-3}$	564	476	0.645	25.9	7.5
$5.18 \times 10^{-3}$	534	449	0.612	31.5	7.4
$5.18 \times 10^{-3}$	505	421	0.612	31.5	7.4
$6.7 \times 10^{-3}$	483	398	0.585	36.1	7.8
$6.7 \times 10^{-3}$	477	391	0.585	36.1	7.8
$8.27 \times 10^{-3}$	480	394	0.558	39.6	7.5
$8.27 \times 10^{-3}$	474	388	0.558	39.6	7.5
$8.27 \times 10^{-3}$	440	356	0.558	39.6	7.5

$T_0$  = Measured relaxation times

$T$  = Chemical process relaxation times.

TABLE V  
RELAXATION TIMES AND F(c) FOR NICKEL(II) SUCCINATE ( $\mu \rightarrow 0$ )

$C_0 \times 10^3$ (M)	$T_0 \times 10^3$ (sec) at 17°C	$T \times 10^3$ (sec) at 17°C	$\gamma_{\pm}$	$f(c) \times 10^4$ (M)	$T_0 \times 10^3$ (sec) at 21.5°C	$T \times 10^3$ (sec) at 21.5°C
3.74	436	350	0.645	25.9	350	259
3.74	450	363	0.645	25.9		
3.74	480	394	0.645	25.9		
5.18	415	329	0.612	31.5	324	230
5.18	438	352	0.612	31.5	330	235
5.18			0.612	31.5	324	230
6.7	414	328	0.585	36.1	315	219
6.7	408	320	0.585	36.1	312	216
8.27	405	316	0.558	39.6	306	210
8.27	405	316	0.558	39.6	306	210
8.27			0.558	39.6	300	204

$T_0$  = Measured relaxation times

T = Chemical Process relaxation times

TABLE VI  
RELAXATION TIMES AND  $f(c)$  FOR MAGNESIUM OXALATE AT 12.8°C ( $\mu \rightarrow 0$ )

$C_0(M)$	$T_0(\mu\text{sec})$	$T(\mu\text{sec})$	$\gamma_{\pm}$	$f(c) \times 10^4 (M)$	pH	Electrolyte (KCl) ( $M \times 10^3$ )
$1.6 \times 10^{-3}$	282	196	0.79	9.00	6.2	5.2
$1.6 \times 10^{-3}$	288	202	0.79	9.00	6.2	5.2
$1.6 \times 10^{-3}$	276	189	0.79	9.00	6.2	5.2
$1.0 \times 10^{-3}$	326	241	0.82	7.02	7.0	3.3
$1.0 \times 10^{-3}$	340	255	0.82	7.02	7.0	3.3
$6 \times 10^{-4}$	360	277	0.85	5.13	6.6	1.9
$6 \times 10^{-4}$	383	301	0.85	5.13	6.6	1.9

$T_0$  = Measured relaxation times

$T$  = Chemical process relaxation times

TABLE VII  
RELAXATION TIMES AND  $F(c)$  FOR MAGNESIUM OXALATE ( $\mu \rightarrow 0$ )

$C_0(M)$	$T_0(\mu\text{sec})$ at 18.5°C	$T(\mu\text{sec})$ at 18.5°C	$f(c) \times 10^4$ (M)	$\gamma_{\pm}$	$T_0(\mu\text{sec})$ at 23.5°C	$T(\mu\text{sec})$ at 23.5°C
$1.6 \times 10^{-3}$	204	116	9.00	0.79	202	114
$1.6 \times 10^{-3}$	216	128	9.00	0.79	196	108
$1.6 \times 10^{-3}$	235	147	9.00	0.79	188	100
$1.0 \times 10^{-3}$	250	162	7.02	0.82	210	122
$1.0 \times 10^{-3}$	255	167	7.02	0.82	228	140
$1.0 \times 10^{-3}$	268	181	7.02	0.82	233	144
$6 \times 10^{-4}$	300	214	5.13	0.85	264	177
$6 \times 10^{-4}$	300	214	5.13	0.85	259	172
$6 \times 10^{-4}$	296	210	5.13	0.85		

$T_0$  = Measured relaxation times

$T$  = Chemical process relaxation times

By measuring the relaxation time (Table I to Table VII) for different values of  $f(c)$  at three different temperatures,  $k_f$  was calculated and the values obtained are shown in Tables VIII, IX, and X.

Equation (IV-5), rather than (II-19), was used to calculate  $k_f$ , because the effect of the concentration on  $k_{34}'$  which had been illustrated in Chapter II was considered. Since very dilute equilibrium concentrations were used for the magnesium oxalate and the nickel(II) malonate systems, the concentration effect on  $k_{34}'$  may be neglected. A plot (Figure 12 and 13) of the concentrations against the reciprocal of the relaxation times gives  $k_f$  and  $k_r$ . The  $k_f/k_r$  ratios are in good agreement with the independently determined stability constants obtained from the literature and  $k_f$  is consistent with that evaluated from equation (IV-5).

Values of Arrhenius energies of activation for the reaction process of the malonate and succinate systems have been calculated from the slopes of plots of  $\log k$  against  $\frac{1}{T} \times 10^3$ . The entropies of activation,  $\Delta S_f^*$ , enthalpies of activation,  $\Delta H_f^*$ , and free energy of activation,  $\Delta G_f^*$ , were obtained from the equations:

$$\Delta H^* = E_f - RT \quad (\text{II-31})$$

$$\ln A = \ln \frac{eRT}{Nh} + \frac{\Delta S^*}{R} \quad (\text{II-33})$$

$$\Delta G^* = \Delta H^* - T\Delta S^* \quad (\text{IV-6})$$

where  $\ln A$  is the intercept obtained from the Arrhenius plots. The linearity of the plots, as shown in Figure 14, suggests that the above

FIGURE 12  
CONCENTRATION DEPENDENCE OF THE RELAXATION TIME  
FOR NICKEL MALONATE

G = at 32.5°C

S = at 23.5°C

U = at 14.5°C

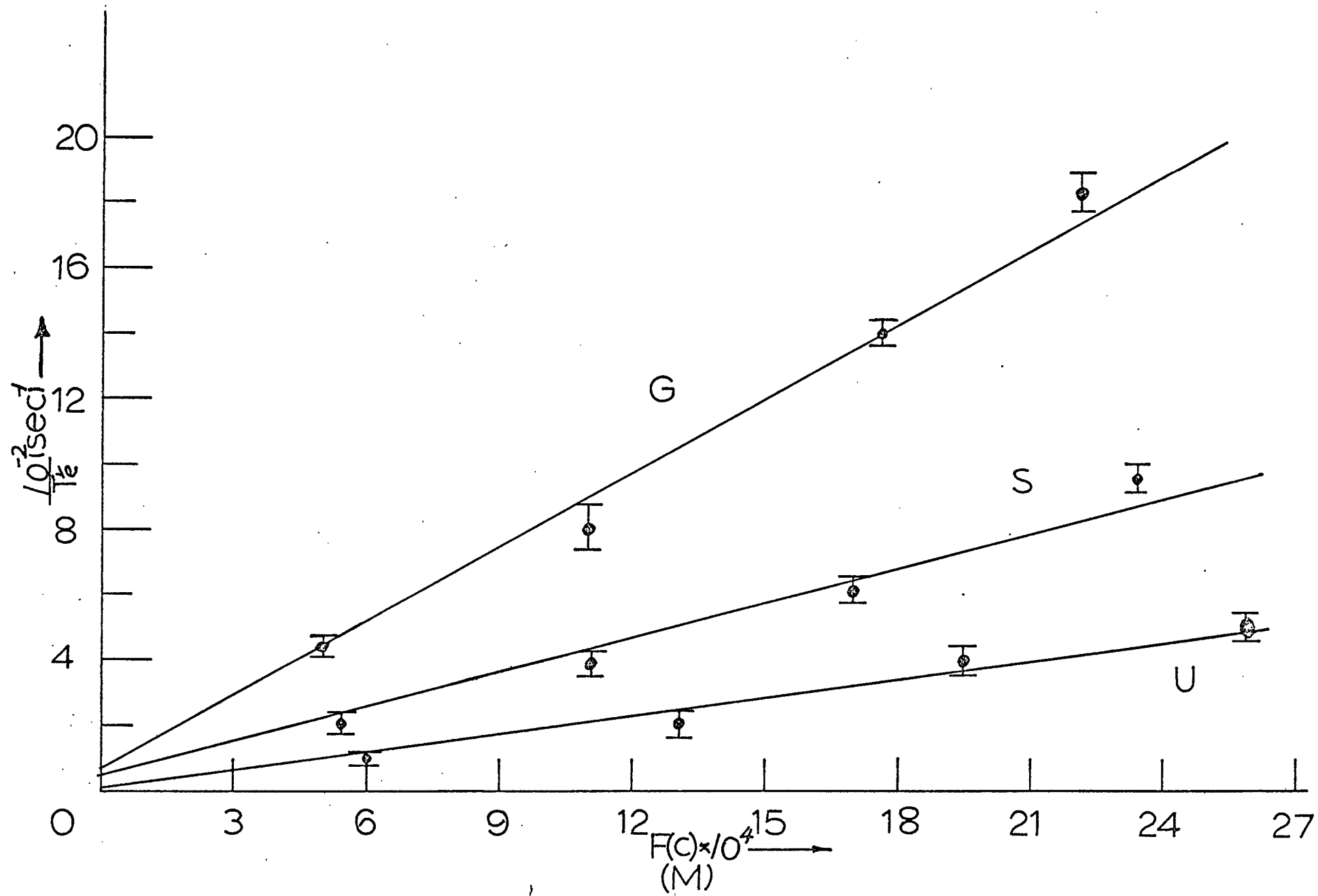
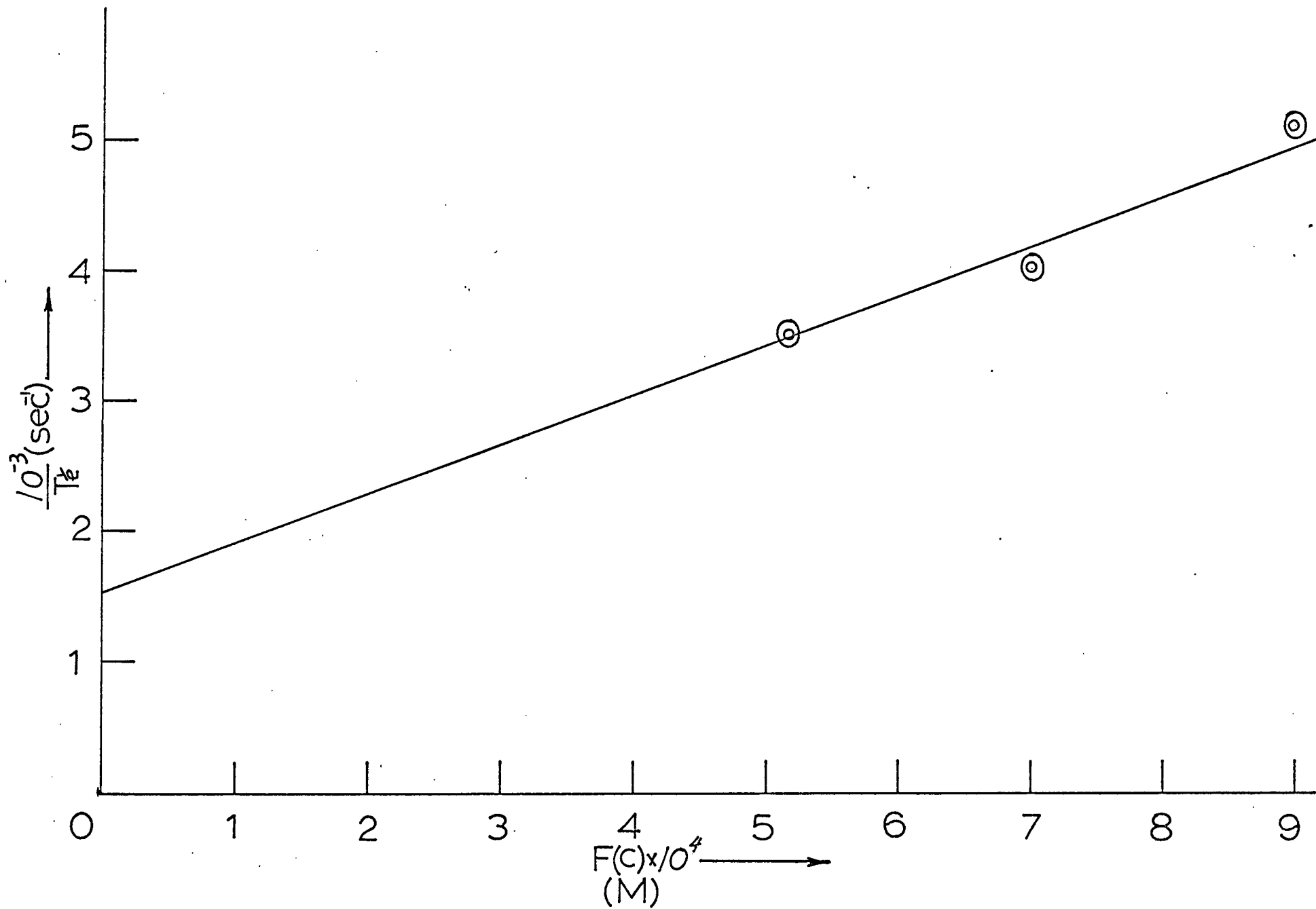


FIGURE 13  
CONCENTRATION DEPENDENCE OF THE RELAXATION TIME  
FOR MAGNESIUM OXALATE AT 13°C



## FIGURE 14

THE TEMPERATURE DEPENDENCE OF  $k_f$

A = The Nickel Malonate System

C = The Nickel Succinate System

S = The Magnesium Oxalate System

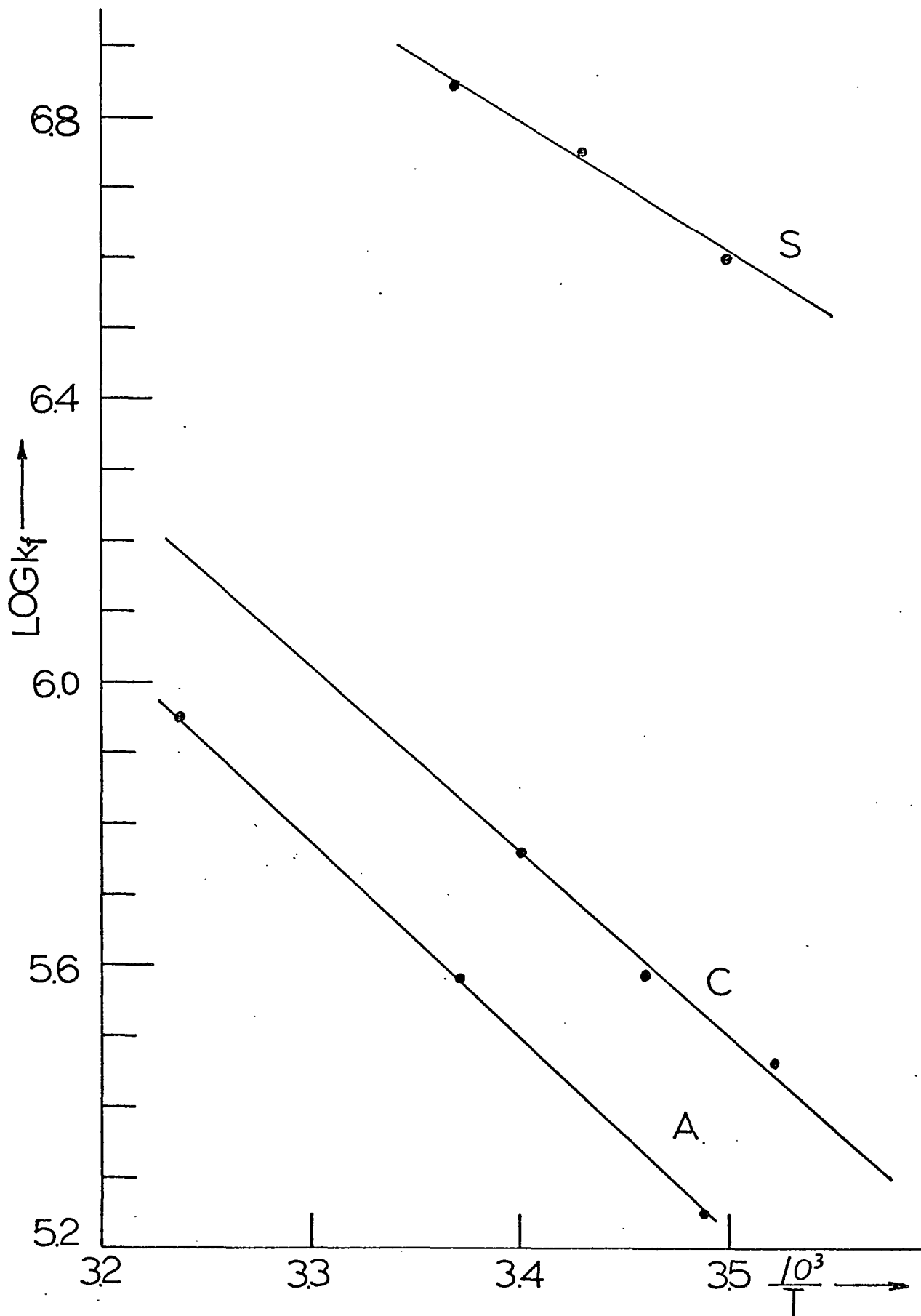


TABLE VIII  
RATE CONSTANTS AND  $C_0$  FOR NICKEL(II) MALONATE

$C_0$ (M)	$k_f \times 10^{-5}$ at 14.5°C ( $M^{-1} \text{sec}^{-1}$ )	$k_f \times 10^{-5}$ at 23.5°C ( $M^{-1} \text{sec}^{-1}$ )	$k_f \times 10^{-5}$ at 32.5°C ( $M^{-1} \text{sec}^{-1}$ )
$1.6 \times 10^{-3}$	1.45	3.53	7.45
$1.6 \times 10^{-3}$	1.45	3.53	7.76
$8 \times 10^{-3}$	1.55	3.42	7.28
$8 \times 10^{-3}$	1.46	3.20	7.42
0.02	2.08	3.83	7.66
0.02	2.04	3.83	7.5
0.04	2.04	4.27	9
0.04	1.96	4.67	
Average	1.75	3.78	7.72

TABLE IX  
RATE CONSTANTS AND F(c) FOR NICKEL(II) SUCCINATE

$f(c) \times 10^4 (M)$	$k_f \times 10^{-5}$ at 125°C ( $M^{-1} \text{sec}^{-1}$ )	$k_f \times 10^{-5}$ at 17°C ( $M^{-1} \text{sec}^{-1}$ )	$k_f \times 10^{-5}$ at 21.5°C ( $M^{-1} \text{sec}^{-1}$ )
25.9	2.7	3.86	5.54
25.9	2.7	3.72	
25.9		3.43	
31.5	2.8	3.92	5.76
31.5	2.98	3.66	5.9
31.5			5.76
36.1	2.96	3.62	5.9
36.1	3.02	3.7	5.97
36.1			
39.6	2.96	3.8	5.9
39.6	3.0	3.8	5.9
39.6	3.26		6.06
Average	2.94	3.78	5.85

TABLE X  
RATE CONSTANTS AND F(c) FOR MAGNESIUM OXALATE

$f(c) \times 10^4 (M)$	$k_f \times 10^{-6}$ at 12.8°C (M <sup>-1</sup> sec <sup>-1</sup> )	$k_f \times 10^{-6}$ at 18.5°C (M <sup>-1</sup> sec <sup>-1</sup> )	$k_f \times 10^{-6}$ at 23.5°C (M <sup>-1</sup> sec <sup>-1</sup> )
9	4.01	6.78	6.9
9	3.9	5.75	7.28
9	4.16	5.35	7.87
7.02	3.88	5.78	7.67
7.02	3.68	5.69	6.67
7.02		5.17	6.6
5.13	4.11	5.33	6.43
5.13	3.78	5.33	6.64
5.13		5.43	
Average	3.97	5.62	7.01

assumption is valid for the temperature range investigated. The uncertainties in  $E_f$  and  $\Delta S_f^*$  for the nickel system are about  $\pm 0.6$  kcal and  $\pm 2.1$  cal deg $^{-1}$ mole $^{-1}$ ; for the magnesium system Mgox  $\pm 1.0$  kcal and  $\pm 2$  cal deg $^{-1}$ mole $^{-1}$ .

In these calculations,  $\Delta S_0$  was assumed to be equal to  $-19.4 \frac{Z-Z+}{a}$  (10,11) with  $a$ , the distance of closest approach of the ion pair partners, equal to  $5A$  (24) (approximately the internuclear distance of a coordinate bond plus the effective thickness of a water molecule);  $Z_-$  and  $Z_+$  are the charges on the metal ion and the ligand, respectively.

The enthalpy change for the first two steps was obtained from the relationship

$$\Delta H_0 = -RT \ln K_0 + T\Delta S_0 \quad (IV-7)$$

The other parameters are defined by

$$\Delta H_{34}^* = \Delta H_f^* - \Delta H_0 \quad (IV-8)$$

and

$$\Delta S_{34}^* = \Delta S_f^* - \Delta S_0 \quad (IV-9)$$

A change in  $K_0 = K_a K_b$  by a factor of 2 or 3 will result in about a 20% and 5% variation in  $\Delta H_0$  and  $\Delta H_{34}^*$ , respectively. This will also result in about 10% variation in  $k_f$  for the dilute solutions used in this experiment and will have the same order of magnitude variation in  $k_{34}$  values.

The equilibrium constant,  $K_a$ , for the first step has been estimated by Eigen and Tamm (8) from a theory based on simple Coulombic interaction as  $K_a = 25-40$ . This value should be the same for any di-divalent electrolyte. No theoretical estimate is available for  $K_b$ . In the interpretation of the ultrasonic relaxation values of  $K_b$  range from 0.5 to 1. In 1964, Pottel (25) came to essentially the same conclusions on the basis of the presence of three types of ion associates as well as free hydrated ions.

Another approximation of this constant ( $K_0$ ) can be obtained by using Bjerrum ion-pair constant (26,27) or its diffusion theory equivalent (12). The results for spherically symmetric ions can be expressed as

$$K_0 = \frac{4\pi a^3}{3000} e^{-\mu(a)KT} \quad (IV-8)$$

$$\mu(a) = \frac{z_1 z_2 e^2}{aD} - \frac{z_1 z_2 e^2 k}{D(1 + ka)} \quad (IV-9)$$

$$k^2 = \frac{8\pi N e^2}{1000 DKT} \mu \quad (IV-10)$$

where  $\mu$  is the ionic strength,  $N$  is Avogadro's number,  $a$  is the distance of closest approach of the ion pair partner,  $z$  is the charge on the  $i$ th ion,  $e$  is the electron charge,  $KT$  is the Boltzmann energy factor, and  $D$  is the dielectric constant of the solvent.

The resulting values of  $K_0$  calculated from these equations are probably valid within a factor of two or three. Here the value of the rate constants,  $k_{34}$ , was estimated by assuming  $K_0 = K_a K_b = 25$ .

The values of  $k_{34}$  for the nickel monomalonate and monosuccinate complexes determined in this way are quite similar and are of the same order of magnitude as values obtained for other systems, as is shown in Table XI. Since the values of  $k_{34}$  for the various ligands of the nickel(II) system are about the same and because of the experimental errors involved, it is difficult to show any ligand effect in the rate of complex formation. It appears that the loss of the first water is the rate determining step and is insensitive to the environment produced by the anion in the ion pair complex. The parameters shown in Tables XII and XIII are almost the same, within experimental error, for the nickel malonate and succinate systems.

A comparison of the results of this investigation and other reported rate data on bidentate ligands with other studies indicates that the formation of the second ligand metal bond does not noticeably affect the measured rate constant. Including the last step, the forward rate constant is given by the relationship

$$k_f = \frac{K_a K_b k_{34} k_{45}}{k_{43} + k_{45}} \quad (\text{IV-11})$$

and the reverse rate constant by

$$k_r = \frac{k_{43} k_{54}}{k_{43} + k_{45}} \quad (\text{IV-12})$$

Since the rate is insensitive to the second metal ligand bond formation, then  $k_{45}$  must be much faster than  $k_{43}$ ; in other words, the complex

TABLE XI  
 RATE CONSTANTS  $k_{34}$  FOR THE FORMATION OF INNER-SPHERE  
 COORDINATION COMPLEXES BETWEEN NICKEL AND VARIOUS LIGANDS

Ligand	Temp (°C)	Ionic Strength (M)	$k_{34} \times 10^{-4} (\text{sec}^{-1})$	Reference
Sulfate	20	0	1.5	(9,12)
Glycine	25	0.15	0.9	(24)
Diglycine	25	0.15	1.2	(24)
Triglycine	25	0.1	0.5	(28)
Imidazole	25	0.15	1.6	(24)
Malonate	25	0	~ 2	(29)
Amine	25	0.1	3	(30)
Malonate	23.5	~ 0	1.5	This work
Succinate	21.5	~ 0	2.3	This work

TABLE XII  
KINETIC DATA FOR THE NICKEL(II) MALONATE FORMATION AT 23.5°C ( $\mu \rightarrow 0$ )

$\text{Ni}^{2+} + \text{Mal}^{2-} \xrightleftharpoons[k_r]{k_f} \text{NiMal}$	
$k_{eq}$	$1.23 \times 10^4$
$k_f(\text{M}^{-1}\text{sec}^{-1})$	$3.8 \times 10^5$
$k_r(\text{sec}^{-1})$	31
$E_f(\text{kcal M}^{-1})$	14.2
$\Delta H_f^*(\text{kcal M}^{-1})$	13.7
$\Delta S_f^*(\text{cal deg}^{-1}\text{M}^{-1})$	12.7
$\Delta G_f^*(\text{kcal M}^{-1})$	9.4
$K_o = K_a K_b$	25
$k_{34}(\text{sec}^{-1})$	$1.5 \times 10^4$
$\Delta G_o(\text{kcal M}^{-1})$	-1.9
$\Delta S_o(\text{cal deg}^{-1}\text{M}^{-1})$	15
$\Delta H_o(\text{kcal M}^{-1})$	2.7
$\Delta H_{34}^*(\text{kcal M}^{-1})$	11
$\Delta S_{34}^*(\text{cal deg}^{-1}\text{M}^{-1})$	-2.3

TABLE XIII

KINETIC DATA FOR THE NICKEL(II) SUCCINATE FORMATION AT 21.5°C ( $\mu \rightarrow 0$ )

$\text{Ni}^{2+} + \text{Suc}^{2-} \xrightleftharpoons[k_r]{k_f} \text{NiSuc}$	
Keq	$2.14 \times 10^2$
$k_f (\text{M}^{-1} \text{sec}^{-1})$	$5.8 \times 10^5$
$k_r (\text{sec}^{-1})$	$2.7 \times 10^3$
$E_f (\text{kcal M}^{-1})$	14
$\Delta H_f^* (\text{kcal M}^{-1})$	13.5
$\Delta S_f^* (\text{cal deg}^{-1} \text{M}^{-1})$	13.4
$\Delta G_f^* (\text{kcal M}^{-1})$	9
$K_0 = K_a K_b$	25
$k_{34} (\text{sec}^{-1})$	$2.3 \times 10^4$
$\Delta G_0 (\text{kcal M}^{-1})$	-1.9
$\Delta S_0 (\text{cal deg}^{-1} \text{M}^{-1})$	15
$\Delta H_0 (\text{kcal M}^{-1})$	2.7
$\Delta H_{34}^* (\text{kcal M}^{-1})$	10.8
$\Delta S_{34}^* (\text{cal deg}^{-1} \text{M}^{-1})$	-1.6

is much more likely to form the bidentate complex than to revert to the ion pair which simplifies the expression for the forward rate constant to

$$k_f = K_a K_b k_{34} \quad (IV-13)$$

In summary, no noticeable effect was found in the forward rate constant and activation parameters due to changing the ligand from malonate to succinate.

The same procedure was used to calculate the kinetic data for the magnesium oxalate system; these data are summarized in Table XIV. The rate constants and enthalpies of activation are tabulated in Table XV, which also includes a comparable set of data for the reactions of the metal ion with dye, oxalate, malonate, succinate, and water exchange. There are three points to be noted. First of all, not only the rate constants ( $k_{34}$ ), but also the big enthalpies of activation ( $\Delta H_{34}^*$ ) which have something to do with bond breaking of the water molecule from a given metal ion are quite similar. These results again show that the rate-limiting step is the third one and the rate constant of this step is controlled primarily by the change in enthalpy of activation. Secondly, the rate of complex formation from hydrated divalent ions is mostly characteristic of the metal-aquo ion, the reverse reaction ( $k_r$ ), the dissociation of the complex contains the specific influences of the ligands; in other words, the forward free energies of activation depend on the metal ions, but the reverse free energies of activation depend upon the ligands, since they have different stability constants for a given metal ion with different

TABLE XIV  
KINETIC DATA FOR THE MAGNESIUM OXALATE FORMATION AT 12.8°C ( $\mu \rightarrow 0$ )

$\text{Mg}^{2+} + \text{Ox}^{2-} \xrightleftharpoons[k_r]{k_f} \text{Mgox}$	
Keq	$2.7 \times 10^3$
$k_f (\text{M}^{-1} \text{sec}^{-1})$	$3.97 \times 10^6$
$k_r (\text{sec}^{-1})$	$1.47 \times 10^3$
$E_f (\text{kcal M}^{-1})$	9.35
$\Delta H_f^* (\text{kcal M}^{-1})$	8.75
$\Delta S_f^* (\text{cal deg}^{-1} \text{M}^{-1})$	2.5
$\Delta G_f^* (\text{kcal M}^{-1})$	8.04
$K_o = K_a K_b$	25
$k_{34}$	$1.6 \times 10^5$
$\Delta G_o (\text{kcal M}^{-1})$	-1.9
$\Delta S_o (\text{cal deg}^{-1} \text{M}^{-1})$	15
$\Delta H_o (\text{kcal M}^{-1})$	2.4
$\Delta H_{34}^* (\text{kcal M}^{-1})$	6.35
$\Delta S_{34}^* (\text{cal deg}^{-1} \text{M}^{-1})$	-12.5

TABLE XV  
SUBSTITUTION OF INNER-SPHERE AQUO COMPLEXES

Metal ion Ligand	Conditions	$r(\text{\AA})$	$k_{34}(\text{sec}^{-1})$	$k_r(\text{sec}^{-1})$	$\Delta H_{34}^*$ (kcal M <sup>-1</sup> )	Method (reference)
Ni <sup>++</sup> , Mal <sup>=</sup>	23.5°C, $\mu \rightarrow 0$	0.78	$1.5 \times 10^4$	31	11	Pressure-jump (This work)
Ni <sup>++</sup> , Suc <sup>=</sup>	21°C, $\mu \rightarrow 0$	0.78	$2.3 \times 10^4$	$2.7 \times 10^3$	10.8	Pressure-jump (This work)
Ni <sup>++</sup>	25°C	0.78	$2.7 \times 10^4$	-----	11.6	NMR (31)
Co <sup>++</sup>	25°C	0.78	$1.1 \times 10^6$	-----	8.0	NMR (31)
Co <sup>++</sup> , Dye	15°C, $\mu = 0.1$	0.78	$4 \times 10^5$ (a)	7	8.6 (b)	Temperature-jump (32)
Co <sup>++</sup> , SO <sub>4</sub> <sup>=</sup>	20°C, $\mu = 0.1$	0.78	$3 \times 10^5$	$2.5 \times 10^6$	-----	Sound Absorption (12)
Mg <sup>++</sup> , CrO <sub>4</sub> <sup>=</sup>	20°C, $\mu = 0.1$	0.65	$1 \times 10^5$	$1 \times 10^6$	-----	Sound Absorption (12)
Mg <sup>++</sup> , Ox <sup>=</sup>	13°C, $\mu \rightarrow 0.1$	0.65	$1.6 \times 10^5$	$1.5 \times 10^3$	6.4	Pressure-jump (This work)

Mal = Malonate, Suc = Succinate, Ox = oxalate

Dye = pyridine-2-azo-p-dimethylamiline

a = This value was corrected by ion-pair formation stability constant

b = This value was corrected by ion-pair formation and  $\Delta S_0$  was assumed equal to  $\frac{-19.4Z_- Z_+}{a}$ .

ligands. Thirdly, Connick and his co-workers (31) reported the lower rate for nickel(II) than for manganese(II) can probably be attributed to crystal-field effects is again confirmed, because the change in CFSE is added to the activation energy for the process which, in turn, increases the forward free energy of activation, thus decreases the rate of reaction.

All the activation entropy changes (Table XVI) of the rate-determining step are negative except that of the manganese(II) ion. The change of activation entropy can give information about the nature of the reaction, for example, the  $S_N1$  mechanism in aqueous solution studied at high pressure will generally be associated with a large decrease in volume of activation and entropy of activation.

The large volume decrease is due to the separation of ions of the opposite sign. There is an intensification of the electric field and, therefore, an increase in electrostriction. In other words, water molecules will adhere to the ions more closely than to the neutral molecules (33). Since the entropy change is the measurement of the ordering of solution, it seems reasonable to say the large entropy decrease is caused by an increased ordering of the solvent molecules. The same principle can be applied on the outer-sphere and inner-sphere complexes. A more favorable entropy change will be expected for the formation of an inner-sphere complex than a corresponding outer-sphere complex (34), even though this entropy change is thermodynamic rather than kinetic in nature. Perrin (35) pointed out there is a fairly good linear correlation between volumes and entropies of activation; in addition, the volume change resulting from

TABLE XVI  
ENTROPIES OF ACTIVATION OF THE RATE-LIMITING STEP

Metal ion, Ligand	$\Delta S_{34}^*(\text{Cal deg}^{-1}\text{M}^{-1})$	$\gamma(A)^{(c)}$	Method (reference)
Mg <sup>++</sup> , Ox <sup>=</sup>	-12.5(13°C)	0.65	Pressure-jump (This work)
Ni <sup>++</sup> , Mal <sup>=</sup>	-2.3(23°C)	0.78	Pressure-jump (This work)
Ni <sup>++</sup> , Suc <sup>=</sup>	-1.6(21°C)	0.78	Pressure-jump (This work)
Mn <sup>++</sup>	2.2(25°C)	0.80	NMR (31)
Cu <sup>++</sup>	-4(25°C)	0.69	NMR (31)
Co <sup>++</sup>	-4.1(25°C)	0.78	NMR (31)
Fe <sup>++</sup>	-3(25°C)	0.76	NMR (31)

(c) Table of periodic properties of the elements, Dyna-Slide Co.

reorganization of the solvent molecules is generally more important than the structural effect for reactions in which ions or fairly strong dipoles are concerned (36-40).

Considering the high uncertainty found in the measured changes in activation entropy (the errors in  $\Delta S_Q$  are about 4 e.u. for  $Mn^{+2}$ ,  $Cu^{+2}$ ,  $Co^{+2}$ ,  $Fe^{+2}$ , and 2 e.u. for  $Ni^{+2}$ ,  $Mg^{+2}$ , respectively), and the theoretical equation used to calculate the entropy change for the ion pair formation in infinitely dilute solution (41), no definite conclusion can be drawn concerning the nature of the exchange process simply from the changes in activation entropy shown in Table XVI. However, a reasonable explanation for the activation entropy changes according to the proposed mechanism seems to be in fair agreement with the experimental values. The first two steps of the substitution reaction, the formation of ion pairs is expected to have large net increase in entropy due to extensive disruption of the hydration sphere despite the neutralization of electrical charge and more ordering of the free ions. The third step is the dissociation of the first water molecule. Although the release of one water molecule will cause an increase in the disorder of the system or activation energy, it would be compensated for by the formation of the large second and higher coordination spheres owing to the increase in the ratio of charge to radius of the metal ion and its first hydration layer. The smallest ion,  $Mg^{++}$ , seems to be more heavily solvated after losing a water molecule than any other ions due to a bigger change in this ratio. For the largest ion,  $Mn^{++}$  seems still to be dominated by the elimination of a water molecule. This discussion is only qualitative and there are large ex-

perimental errors. Thus, to study the reaction mechanism, the volume changes which depend to a much greater extent on electrostricten effects than on any other effects should be determined as suggested by Whalley (42). However, the purpose of this study has been achieved; that is, the rate-determining step has been found and the mechanism has been proved.

## REFERENCES

1. Eigen, M. and DeMaeyer, L., "Technique of Organic Chemistry," VIII, part 2, "Investigation of Rates and Mechanisms of Reactions," Friers, S., Lewis, E., and Weissberger, A., eds., Interscience, New York (1963).
2. Czerlinski, G. and Eigen, M., Z. Elektrochem., 63, 652 (1959).
3. Strehlow, H. and Becker, M., Z. Elektrochem., 63, 457 (1959).
4. Ljunggren, S. and Lamm, O., Acta Chem. Scand., 12, 1834 (1958).
5. Tamm, K., Z. Elektrochem., 64, 73 (1960).
6. Kirschner, "Advances in the Chemistry of the Coordination Compounds," The MacMillan Company, New York (1961).
7. Diebler, H. and Eigen, M., Z. Physik. Chem., N. F., 20, 299 (1959).
8. Eigen, M. and Tamm, K., Z. Elektrochem., 66, 93 (1962).
9. Eigen, M. and Tamm, K., Z. Elektrochem., 66, 107 (1962).
10. Nancollas, G. H. and Sutin, N., Inorg. Chem., 3, 360 (1964).
11. Cavasino, F. P., J. Phys. Chem., 69, 4380 (1965).
12. Eigen, M., Z. Elektrochem., 64, 115 (1960).
13. Eigen, M., Kurtze, G., and Tamm, K., Z. Elektrochem., 57, 103 (1953).
14. Eigen, M. and Hammes, G. G., J. Am. Chem. Soc., 82, 5951 (1960).
15. Stuehr, J. and Yeager, E., "Physical Acoustics," Vol II, Chapter 6, Mason, W., ed., Academic Press, New York (1964).
16. Caldin, E. F., "Fast Reactions in Solution," John Wiley and Sons, N. Y. (1964).
17. Yankwich, P. E. and Zavitsanos, P. D., J. Phys. Chem., 69, 442 (1965).
18. Flaschka, H. A., "EDTA Titrations," Pergamon Press, New York (1959).
19. Davis, C. W., Trans Faraday Soc., 23, 351 (1927).

20. Nair, V. S. K. and Nancollas, G. H., J. Chem. Soc., 4367 (1961).
21. McAuley, A. and Nancollas, G. H., J. Chem. Soc., 4458 (1961).
22. Davis, C. W., "Ion Association," Butterworths, London (1962).
23. Tamm, T., "Handbuch der Physik," Akustik, I, Flugge, S., ed., Springer, Berlin (1961).
24. Hammes, G. G. and Steinfeld, J. I., J. Am. Chem. Soc., 84, 4639 (1962).
25. Pottel, "Transactions of the Symposium on Electrolytes," John Wiley and Sons, in press (1964).
26. Harned, H. and Owen, B., "The Physical Chemistry of Electrolytic Solutions," Reinhold Publishing Co., New York, N. Y. (1950).
27. Fuoss, R., Connick, R. and Coppel, C., J. Am. Chem. Soc., 80, 2961 (1958).
28. Steinfeld, J. I. and Hammes, G. G., J. Phys. Chem., 67, 528 (1963).
29. Hoffmann, Heinz, Stuehr, J., and Yeager, E., Office of Naval Research, U.S. Department of Commerce, Technical Report 27 (1964).
30. Rorabacher, D. B., Inorg. Chem., 5, 1891 (1966).
31. Swift, T. J. and Connick, R. E., J. Chem. Phys., 37, 307 (1962).
32. Wilkins, R. G., Inorg. Chem., 3, 520 (1964).
33. Laidler, K. J., "Chemical Kinetics," McGraw-Hill Book Company, N. Y., (1965).
34. Lewis, J. and Wilkins, R. G., "Modern Coordination Chemistry," Interscience Publication Inc., New York (1960).
35. Perrin, M. W., Trans Faraday Soc., 34, 144 (1938).
36. Evans, M. G., and Polanyi, M., *ibid.*, 31, 875 (1935).
37. Evans, M. G. and Polanyi, M., *ibid.*, 32, 1333 (1936).
38. Evans, M. G., *ibid.*, 34, 49 (1938).
39. Buchanan, J. and Hamann, S. D., *ibid.*, 49, 1425 (1953).
40. Burris, C. T. and Laidler, K. J., *ibid.*, 51, 1497 (1955).

41. Frost, A. A. and Pearson, R. G., "Kinetics and Mechanism," John Wiley and Sons., Inc., New York, London (1953).
  42. Whalley, E., *ibid*, 55, 798 (1959).
-